PCCP

Emerging trends in the dynamics of polyelectrolyte complexes

Journal:	*Physical Chemistry Chemical Physics*
Manuscript ID	CP-PER-07-2020-003696.R1
Article Type:	Perspective
Date Submitted by the Author:	19-Sep-2020
Complete List of Authors:	Manoj Lalwani, Suvesh; Texas A&M University College Station Eneh, Chikaodinaka; Texas A&M University College Station Lutkenhaus, Jodie; Texas A&M University,

ARTICLE

Emerging trends in the dynamics of polyelectrolyte complexes

Suvesh Manoj Lalwani,[a†] Chikaodinaka I. Eneh[a†] and Jodie L. Lutkenhaus*[ab]

Received 00th January 20xx,
Accepted 00th January 20xx

DOI: 10.1039/x0xx00000x

Polyelectrolyte complexes (PECs) are highly tunable materials that result from the phase separation that occurs upon mixing oppositely charged polymers. Over the years, they have gained interest due to their broad range of applications such as drug delivery systems, protective coatings, food packaging, and surface adhesives. In this review, we summarize the structure, phase transitions, chain dynamics, and rheological and thermal properties of PECs. Although most literature focuses upon the thermodynamics and application of PECs, this review highlights the fundamental role of salt and water on mechanical and thermal properties impacting the PEC's dynamics. A special focus is placed upon experimental results and techniques. Specifically, the review examines phase behaviour and salt partitioning in PECs, as well as different techniques used to measure diffusion coefficients, relaxation times, various superpositioning principles, glass transitions, and water microenvironments in PECs. This review concludes with future areas of opportunity in fundamental studies and best practices in reporting.

1.Introduction

As early as 1929, Bungenberg de Jong *et al.* discovered that oppositely charged polymers spontaneously phase separate upon mixing.[1, 2] Since then, many years of research now show that this complexation process may result in solid-liquid or liquid-liquid phase separation.[3-6] These solid-like "precipitates" and liquid-like "coacervates" have been found in nature as membrane-less organelles[7] and natural adhesives from seaworms,[8] as well as in synthetic systems. The proposed applications of polyelectrolyte complexes (PECs) have ranged widely from energy and health to packaging and reconfigurable materials.[9, 10] These materials have received notable interest because of their tunable properties, resulting from structural changes in response to salt concentration, charge density, pH, and temperature.[4, 11-13]

In recent years, there has been growing interest in the dynamics and rheology of PECs. The multifaceted nature of these materials has provided a rich landscape for fundamental studies on polyelectrolyte chain diffusion, relaxation of PECs, and their viscoelastic response. The overarching challenge for researchers is to connect these observed properties with the highly complicated structure of the PEC. Specifically, a PEC consists of four components: polycation, polyanion, salt, and water; together, these components – as further influenced by pH, temperature, and time-scale of observation – control the number, timescale, and strength of ion pair 'crosslinks". The problem of understanding the dynamics of PECs becomes quickly "complex" when one considers these numerous internal and external factors.

Here, we review the dynamics of PECs as it relates to PEC structure under the lens of current and recent literature. The reader is referred elsewhere to other reviews in consideration of thermodynamics, rheology, and applications.[14-16] A special focus upon experimental approaches is highlighted- particularly with regard to experimental approaches to observing diffusion coefficients, relaxation times, various superpositioning principles, glass transitions, and water microenvironments in PECs.

2. Overview of the polyelectrolyte complex structure

Polyelectrolyte (PE) complexation is driven not only by the electrostatic attraction between the polyanion and polycation but also the entropic "escaping tendency" of counterions upon mixing represented by Equation 1.[17] Additional weaker forces in play are hydrogen bonding and hydrophobic forces.[18, 19]

$$\boldsymbol{Pol^+A^-} + \boldsymbol{Pol^-M^+} \leftrightharpoons \boldsymbol{Pol^+Pol^-} + \boldsymbol{A^-} + \boldsymbol{M^+} \qquad (1)$$

Pol^+ represents a polycation repeat unit, Pol^- is a polyanion repeat unit, Pol^+Pol^- is an intrinsic ion pair, and A^- and M^+ are counterions. Complexation results in the formation of ion pairs that, in turn, determine the complex's structure, properties, and phase (liquid vs. solid). This section examines ion pair effects, simulations of the PEC structure, and PEC phases.

2.1 Extrinsic and intrinsic ion pairing

As shown in **Figure 1**, there are two kinds of ion pairs within a PEC: PE-PE ion pairs (intrinsic ion pairs) and PE-salt ion pairs (extrinsic ion pairs).[12, 20-22] From coarse-grained MARTINI model simulations,[23] it has been reported that intrinsic ion compensations dominates in PEC assemblies. Farhat *et al.* defined the doping level, "y", as the

a. Artie McFerrin Department of Chemical Engineering, Texas A&M University, College Station, Texas 77840, USA
b. Department of Materials Science and Engineering, Texas A&M University, College Station, Texas 77840, USA

† These authors contributed equally
Electronic Supplementary Information (ESI) available: [details of any supplementary information available should be included here]. See DOI: 10.1039/x0xx00000x

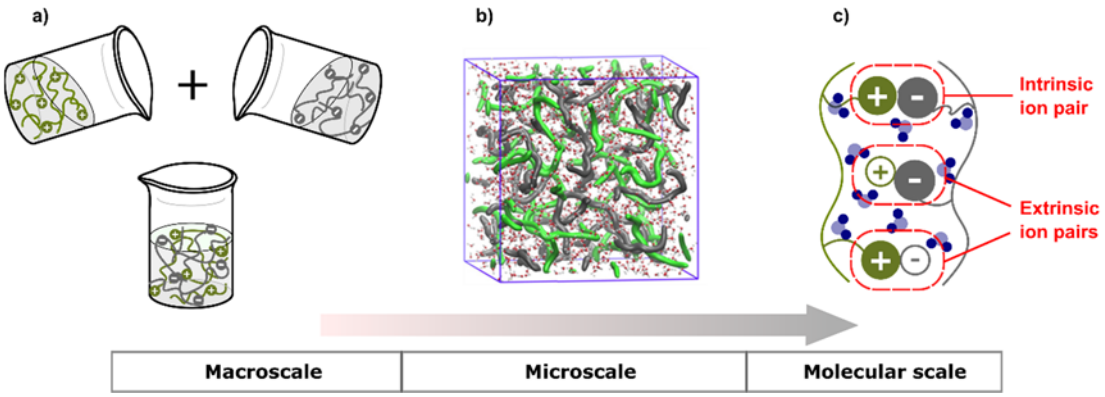

Figure 1: a) Schematic of the preparation of polyelectrolyte complex from polycations and polyanions. b) A representative snapshot of a PAH/PAA complex hydrated with 31.7 wt % water (90% RH) from MD simulations. PAA and PAH backbones are green and gray, respectively. Reprinted with permission from ref. [29]. Copyright 2019 American Chemical Society. c) Schematic of intrinsic (Pol^+Pol^-) and extrinsic (Pol^+A^- or Pol^-M^+) ion pairs

ratio of extrinsic ion pairs to total ion pairs in the PEC.[24, 25] By increasing the ionic strength of the solution environment for already-prepared PECs, intrinsic ion pairs transform into extrinsic ion pairs, resulting in an increase in y.[22, 24, 26-28] For example, a doping level of y = 0 indicates that no extrinsic charge compensation exists, whereas y = 1 indicates that no intrinsic charge compensation exists (*i.e.*, the PEs are unassociated). At a critical salt concentration (c_s) the number of intrinsic ion pairs is not sufficient and the PEC dissociates. This c_s value is strongly dependent on the salt type and the polyelectrolyte system.

The equilibrium presented in Equation 1 may be correlated to the doping level and the ionic strength by the following:

$$K_1 = \frac{y^2}{(1-y)[MA]_{aq}^{\ 2}} \qquad (2)$$

where K_1 is an equilibrium constant that was first experimentally developed from conductivity measurements.[24]

The preceding relationship assumes that the value of y is the same for both the polycation and polyanion. This assumption may breakdown in the case of asymmetric complexes or when one PE is more heavily doped than another. For example, Fu *et al.* showed that there exists a charge imbalance within PECs and polyelectrolyte multilayers (PEMs).[21] An excess of poly(diallyldimethylammonium chloride) (PDADMA) was found in both PDADMA/polystyrene sulfonate (PSS) PECs and PEMs using nuclear magnetic resonance (NMR) spectroscopy.[20, 29] The PEC contained 52-55 mol % PDADMA and the PEM contained 65% PDADMA.[20, 29] This nonstoichiometric composition is due to differences in hydrophobicity and charge density of the two PEs. As a result, the doping level cannot be equal for the two types of extrinsic ion pairs present: PDADMA-Cl and PSS-Na. Accordingly, Zhang *et al.* estimated the cationic (y^+) and anionic (y^-) doping levels of PDADMA/PSS PECs [20] using NMR spectroscopy and neutron activation analysis (NAA). Here, y^+ is the fraction of doped polycation repeat units and y^- is the fraction of doped polyanion repeat units.

Furthermore, the effects of temperature, salt concentration and hydration have been studied using molecular dynamic (MD) simulations of both strong and weak PECs.[6, 30] For a strong PE system, PDADMA/PSS, the contact number of the sulfur atom for PSS and the nitrogen atom for PDADMA was taken as a measure of intrinsic ion pairing. At higher salt molar ratios (defined as a ratio of salt cation to polycation or salt anion to polyanion) and hydration levels, changes in temperature had a more pronounced influence on the number of S-N contacts. At a salt molar ratio of 1.0 and with 26 wt% water present, the number of S–N contacts increased from ~ 1.85 to 2 as temperature increased from 300 – 370 K. Also, as salt molar ratio increased from 0.5 to 1.5, the S–N contact number decreased from 2.3 to 1.6 counts at a fixed hydration of 19 wt%.[6] To summarize, the ionic strength is more influential in determining the number of intrinsic ion pairs, as compared to water or temperature.

For weak polyelectrolyte systems (*i.e.* PEs with pH-dependent degrees of dissociation), the number of intrinsic ion pairs also varies with hydration.[30] MD simulations show that the average number of intrinsic ion pairs per poly(allylamine hydrochloride) PAH repeat unit decreased from 2.32 to 2.0 in PAH/ poly(acrylic acid) (PAA) PECs as relative humidity (RH) increased from 70 – 90 % RH at 20 °C. Similar results were obtained for (PDADMA/PSS) PECs.[6]

2.2 Simulations on polyelectrolyte complex structure: 3D structure and packing

Notably, the preceding simulations reported the average number of intrinsic ion pairs within direct interaction range to be greater than 1 in all conditions. This revelation, in addition to mechanical tests, points to the fact that PECs form complex 3D structures where charged sites are randomly compensated by charged sites from multiple chains, contrary to what most simplified PEC illustrations depict (*i.e.* a perfect one-to-one compensation of two oppositely charged polyelectrolytes in a "ladder" structure**).**[17, 30-33] One study[32] used Monte Carlo simulation to establish that a PEC's structure may range from an ideal ladder to "scrambled egg" based upon the polyelectrolyte chain's stiffness coefficient, ε_{st}. For $\varepsilon_{st} > 30$ (stiff chains), the radius of gyration, R_g, was proportional to chain length (*i.e.*, $R_g \sim n$, where n is the number of repeat units), indicating that the polyelectrolyte chains are highly extended or rigid rods, thus leading to a ladder-type configuration. For $\varepsilon_{st} < 30$ and approaching zero (more flexible chains), R_g scaled as $\sim n^{0.38}$, indicating the polyelectrolyte chains are dense globules, thus leading to a scrambled egg configuration.

MD simulations[20, 30, 34] have revealed that both PDADMA/PSS and PAH/PAA PECs have entangled polyelectrolyte chains with relatively uniform distributions. With more than one intrinsic ion pair

per repeat unit, PAH/PAA PECs form complex three-dimensional structures.[30] These 3-D structures have been confirmed by inspecting an extrinsic ion pair, showing one sodium ion surrounded by multiple PSS groups.[20] Other MD simulations[35] show that polyelectrolytes in solution exhibit a necklace (beads and strings) structure that collapses into one large 3-D bead of complex when neutralized by a complementary polampholyte.

2.3 Phases

Phase separation during complexation is highly dependent on numerous factors, such as polyelectrolyte concentration, mixing ratio, salt concentration, temperature, hydrophobicity, PE molar mass, and pH.[11, 13] Phase separation may result in a polymer-rich liquid coacervate phase, solid precipitate phase, and a polymer-deficient supernatant phase may be obtained.[3, 15, 36] As the doping level y increases for PEMs and PECs, solid precipitates become softer, gradually become viscous liquid-like coacervates, followed by a continued decrease in viscosity, and then eventual disassociation caused by excessive charge screening.[4, 12, 37]

2.3.1 Coacervate/solution theory/boundary

The coacervate/solution boundary is analytically described by the Voorn-Overbeek (VO) theory, which represents one of the earliest and simplest theories to describe coacervation.[38, 39] VO theory combines the Flory Huggins theory of mixing with the Debye-Huckel theory of electrolyte solutions. Thus, the free energy of coacervation, $\boldsymbol{F_{VO}}$, is described by:

$$\frac{F_{VO}}{k_B T} = V\left[\frac{\phi_\pm}{n} ln\, \phi_\pm + (1-\phi_\pm)\ln(1-\phi_\pm) + \chi\phi_\pm(1-\phi_\pm) - \frac{2\sqrt{\pi}}{3}\Gamma^{\frac{3}{2}}\phi_\pm^{\frac{3}{2}}\right] \quad (3)$$

where $\phi_\pm$ is the combined volume fraction of polyelectrolyte, Γ describes the magnitude of electrostatic interaction of electrolyte solution with dielectric constant ϵ and salt ion size a, $\Gamma = e^2/8\pi\epsilon a k_B T$, and χ is the Flory-Huggins solubility parameter

VO theory evaluates the electrostatic attraction between two individual PE coils by treating each one as a charged point following the Debye-Huckel theory.[38] Because this assumption does not always hold true, researchers have developed several other theories and approaches to more accurately describe coacervation.

Jha *et al.*[40] verified VO theory using already-published experimental data of fully ionized PAA/poly(*N*,*N*-dimethylaminoethyl methacrylate) (PDMAEMA) coacervates; they modified VO theory to account for ion sizes and hydrophobic interactions in fitting parameters *l* and χ, assuming uniform salt partitioning. In a follow-up study,[41] the same authors studied the effects of hydrophobicity, pH, salt concentration and polycation to polyanion mixing ratio on coacervation. Hydrophobicity was altered by changing the contacting polycation among PAH, PDADMA and PDMAEMA, and the authors speculated that secondary interactions were responsible for increasing c_s values.

To eliminate the complications of linear charge density mismatch, Lou *et al.* synthesized polyelectrolytes having similar backbone structures from poly(allyl acrylamide).[42] The effects of hydrophobicity were monitored by varying degree of polymerization, n = 50, 100 and 180 while local polarity was varied by oxidizing the sulfide moiety in the polymer chain to different extents. The c_s value increased with increasing N as a result of the reduced translational contribution to entropy of longer polymer chains. The c_s value decreased with increasing local polarity due to the volumetric expansion occurring simultaneously with changes in the sulfide solvation shell as it was oxidized to sulfoxide and sulfone. A modified VO free energy model was used to calculate χ for polymer-water interactions.

Whether the salt partitions preferentially to the coacervate or to the solution phase is a subject of ongoing discussion. VO theory predicts preferential partitioning of salt to the coacervate phase. This was justified by the presence of stronger interactions in the coacervate phase which has a higher charge concentration. In contradiction, experimental and other theoretical studies have instead reported preferential salt partitioning to the supernatant phase.[37, 43-46] Theoretical studies using random phase approximation (RPA)[45, 46] and polymer reference interaction site model (PRISM)[44] both agree with salt partitioning into the supernatant phase. The PRISM-based investigation attributes this expulsion of salt ions to the polymer-deficient phase to the excluded volume of the polymer.[44] Assuming symmetry, Zhang *et al.* affirmed that the excess chemical potential difference between both phases is maintained.[43] For asymmetric systems, however, liquid state (LS) theory predicts that small counterions may be present in either phase, depending on whether there is excess polycation vs polyanion. [47] In addition to salt partitioning behaviour of coacervates, many theoretical approaches have been applied in an attempt to fully understand complex coacervates.[36, 48, 49] These works have been summarized by recent reviews by Sing and Perry. [15, 50]

2.3.2 Coacervate/precipitate theory/boundary

In the absence of salt, solid-liquid phase separation almost always occurs.[4, 11, 13, 41] Solid-like PECs, or precipitates, are typically white, insoluble complex materials. These are stable in most solvents but transform into coacervates when exposed to salt solutions at high ionic strength. Solid-like PECs have been prepared into bulk complexes, multilayer films, microcapsules, micelles and extrudates. So far, turbidity measurements, visual observation, and optical microscopy are the simplest means to identify solid vs liquid PECs.

Turbidity is often used to identify PEC formation, but turbidity cannot distinguish whether a coacervate or a precipitate has been formed. For example, we reported that solid-like PECs exhibited a turbidimetric response, even exhibiting long-term colloidal stability under certain conditions.[11] Specifically, the colloidal stability of PDADMA/PSS PECs over time was explored with varying ionic strength and mixing ratio. Without added salt, precipitates were colloidally stable for days, but upon adding salt, thread-like precipitates formed and settled. At higher salt concentrations (3.0 M), solid precipitates initially formed but then dissolved within a day to form a clear solution. These differences in stability were attributed to variations in the PEC's hydrodynamic size and zeta potential. An important feature of this study is that it indicated the temporal and path-dependent nature of PEC formation. From this result, we caution that one should be careful in preparing PEC phase diagrams using turbidity, because phase separation may vary with time and turbidity cannot distinguish between liquid or solid PECs.

Elsewhere, Salehi *et al.*[41] mapped out the coacervate/precipitate boundary for PDADMA, PDMAEMA and PAH complexes formed with PAA using visual observation. They show that this boundary is more dependent on the mixing ratio than the pH of the polyelectrolytes. The salt concentration for the precipitate/coacervate transition remained slightly above 0 M, confirming that PDADMA/PAA precipitates are formed mainly in the absence of salt. PDMAEMA/PAA showed a slight wider range from pH 4 – 6 where the precipitate/coacervate transition salt concentration was merely 0.25 M. For PAH/PAA, the precipitate/coacervate transition salt concentration was as high as 3 M at pH 5. These differences herein highlight the influence of hydrophobicity and charge density of the polycations used.

Opportunities to map out the coacervate/precipitate boundary using dynamic mechanical analysis (DMA) measurements were suggested by Wang *et al.*[4] In this case, the crossover point between storage modulus ($\boldsymbol{G}'$), loss modulus ($\boldsymbol{G}''$) was investigated as a method of defining this boundary. This, however, is limited by the strong dependence of $\boldsymbol{G}'$ and $\boldsymbol{G}''$ on frequency. Also, the use of one single condition was tentative because there was no change in the slope of the loss modulus and viscosity at the transition.

More recently, Liu *et al.* developed a frequency invariant approach to identify the precipitate/coacervate boundary for PSS/PDADMA complexes doped with KBr.[51] At low salt concentrations, $\boldsymbol{G}' > \boldsymbol{G}''$ for the entire frequency range investigated, indicating solid-like behavior and formation of solid precipitates. At high salt concentrations, $\boldsymbol{G}' < \boldsymbol{G}''$, indicating the formation of coacervates. In addition, tan($\boldsymbol{\delta}$) decreased with increasing frequency for coacervates and vice versa for solid precipitates. Thus, the coacervate-precipitate transition point was identified where tan($\boldsymbol{\delta}$) no longer varied with frequency. This transition salt concentration was identified as 0.85 M KBr.

In preparing this review, we found no theoretical attempts to capture the precipitate/coacervate boundary. This is likely because of the highly complex nature of the two phases, where we speculate that hydrophobic and hydrogen-bonding interactions among polycations, polyanions, water molecules, and salt ions are key factors, rendering such a boundary difficult to model. This idea is supported by a recent study examining the precipitate/coacervate boundary in solvent mixtures of varying hydrophobicity.[52]

3. Polymer chain dynamics within solid- and liquid-like polyelectrolyte complexes

As described in the previous section, salt facilitates the conversion of intrinsic ion pairs to extrinsic ion pairs, which results in increased polyelectrolyte chain dynamics within PECs or PEMs. Because most diffusion measurements in the literature pertain to PEMs, we will restrict our discussion to those. The diffusion coefficient of polyelectrolyte chains within a PEM depends on various factors such as concentration and type of salt, polyelectrolyte system, temperature, molecular weight of the polyelectrolytes, and pH. Additionally, the diffusion of polyelectrolyte chains within a PEM (10^{-12} - 10^{-19} cm^2/sec) is slow in comparison to the diffusion of polyelectrolyte chains in solution (10^{-5} cm^2/sec)[53] due to the presence of intrinsic ion pairs in the PEMs. Here, we summarize experimental observations of polyelectrolyte chain diffusion in PEMs from atomic force microscopy (AFM), neutron reflectometry (NR), fluorescence recovery after photobleaching (FRAP), quartz crystal microbalance with dissipation (QCM-D), radiolabeling, and Fourier transform infrared (FTIR) spectroscopy.[54-67] As we highlight here, each method accesses different aspects of diffusion such as perpendicular vs parallel diffusion and polyelectrolyte chain diffusion vs. extrinsic site diffusion.

3.1 Atomic force microscopy

The earliest measurement of the diffusion of polyelectrolyte chains in PSS/PDADMA PEMs was executed using AFM.[60] Freshly prepared PEMs were annealed in solutions of varying salt concentrations. The surface roughness decreased with increasing salt concentration. The peak to valley dimension Δ was used to estimate the diffusion coefficient, D, as $\Delta = (2Dt)^{\frac{1}{2}}$. Specifically, D was found to be 5×10^{-14} cm^2/sec for the PEM immersed in 1.0 M NaCl solution.

3.2 Fluorescence recovery after photobleaching

The lateral diffusion coefficient in PEMs using fluorescently tagged polyelectrolyte has been measured using FRAP.[54-58] A light source focuses on a small area of the multilayer which causes it to become dark due to irreversible photobleaching. As time proceeds, the dark spot regains fluorescence due to the lateral diffusion of polyelectrolyte chains. Assuming a Gaussian profile for recovery of the fractional fluorescent intensity of the bleached spot, the diffusion coefficient is[68]:

$$D = \frac{\gamma R^2}{4t_{1/2}} \qquad (4)$$

where R is the bleaching spot's radius, γ is the shape factor for the bleaching beam (0.88 for circular beam), and $t_{1/2}$ is the time taken for fractional fluorescent intensity to reach 0.5. In the case of long recovery times, the diffusion coefficient is estimated by the change in shape of the intensity profile of the fractional fluorescence.[58]

Nazaran *et al.* measured the diffusion of fluorescently tagged polyelectrolyte in PEMs composed of PSS/PDADMA.[58] In the last LbL deposition cycle the polycation was replaced by fluorescein-labelled PAH (FITC-PAH) (FITC: Fluorescein isothiocyanate, isomer I). The diffusion coefficient increased by an order of magnitude for preparation salt concentrations of 0.1 M vs 1 M NaCl.[58] In contrast, there was a slight increase in diffusion coefficient for preparation salt concentrations of 0.1 M vs 1 M NaBr. The increase in diffusion coefficient is due to increased electrostatic screening by salt and a decreased number of intrinsic ion pairs. As for salt type, for a low ionic strength preparation solution (0.1 M), the diffusion coefficient increased by a factor of 40 when the salt type was changed from NaCl to NaBr.[58] In contrast, for preparation solutions of high ionic strength (1 M), the effect of salt type was less pronounced. The diffusion coefficient also depends on the polyelectrolyte type. In that same study,[58] the diffusion coefficient of the FITC-labelled PAH increased

from lowest to highest value in PEMs of: PSS/PAH < PSS/PDADMA < HA/PDADMA.

Temperature also influences the diffusion of polyelectrolytes within the PEM. The increase in temperature increases the energy and thus the diffusion coefficient of polyelectrolyte chain. There was a 1-2 order change in magnitude of diffusion coefficient PSS/PDAMA multilayers in water when temperature was raised from 20 ^{o}C to 65 ^{o}C.[58]

Further, the polyelectrolyte's molecular weight influences chain mobility within the PEM. The increase in molecular weight of polyelectrolyte chain leads to an increase in the number of intrinsic ion pairs and/or number of entanglements, thus impacting the diffusion. Xu *et al.* found that the lateral diffusion scaled with M_w^{-1} (molecular weight of polyanion), which signified Rouse-like relaxation.[54] In contrast, Fares *et al.* found that the diffusion coefficients measured using radiolabelling and FTIR spectroscopy were independent of molecular weight of polyanion.[66]

Xu *et al.* compared lateral ($D_{||}$) and perpendicular ($D_{\perp}$) diffusion in PEMs composed of poly(methacrylic acid) (PMAA)/poly(2-(dimethylamino)ethyl methacrylate) and PMAA/quaternized PDMA (Q100M) using FRAP and NR, respectively.[57] $D_{||}$ represents the diffusion of polyelectrolyte chains parallel to the substrate, and $D_{\perp}$ represents diffusion perpendicular to the substrate. For FRAP, PMAA tagged with Alexa fluor 488 was included in the middle of the multilayer to avoid the impact of polymer-water and polymer-substrate influences on diffusion. $D_{||}$ and $D_{\perp}$ both increased with increasing salt concentration of the annealing solution, but $D_{\perp}$was orders of magnitude (4-5) less than $D_{||}$. This suggested that chain diffusion in PEMs is highly anisotropic in nature, perhaps due to the nature of their assembly.

Annealing salt concentration is highly influential on the resulting polyelectrolyte diffusion coefficient. An increase in salt concentration of the annealing solution leads to a decrease in the fraction of intrinsic ion pairs and thus increases the diffusion coefficient of the polyelectrolyte. Selin *et al.* showed that both $D_{\perp}$ and $D_{||}$ scaled exponentially with annealing salt concentration (D$\sim \exp(b[c_{salt}])$) using FRAP.[56] Elsewhere, Jomaa *et al.* proposed a power law model for diffusion and annealing salt concentration ($D \sim D_0[c_{salt}]^{\lambda}$) related to diffusion mediated by the breaking of multiple intrinsic ion pairs.[59] In contrast, Spruijt *et al.* proposed a stretched exponential relationship for chain relaxation ($\tau_c \propto \exp\left(-\sqrt{c_{salt}}\right)$) based upon sticky Rouse dynamics in coacervates from rheological measurements.[69] However, Selin *et al.*[56] discuss that the power law model[59] does not consider changes in dielectric environment with salt concentration, changes in multilayer hydration, or contributions of non-electrostatic interactions to segmental binding; also, the authors[56] were unable to satisfactorily fit the stretched exponential relationship to the data.[69]

Regarding the nature of chain diffusion as it relates to PEM growth, higher mobility was observed in PEMs exhibiting exponential growth as compared to linear growth.[55] Xu *et al.* observed a 5-fold increase in lateral diffusion when the deposition pH during LbL assembly was changed from 4.5 to 6 for PDMA/PMAA and Q100M/PMAA PEMs.[55] These changes in pH caused the PEM growth to shift from linear to exponential regimes because of changes in the ionization of the polyelectrolytes.

3.3 Neutron reflectometry

Neutron reflectometry has been used to measure the diffusion of deuterated polyelectrolyte chains within as-made PEMs by one of two methods. In the first a "limited source" diffusion model was used to estimate diffusion from changes in the concentration of d-PSS with time.[59] In the second, the diffusion coefficient was estimated from changes in the interfacial roughness of deuterated layers.[57]

Jomaa *et al.*[59] measured the diffusion coefficient of deuterated PSS (d-PSS) within PDADMA/PSS PEMs during post-assembly salt annealing with 0.8 M NaCl with the help of NR to measure $D_{\perp}$, as described in the preceding section. The PEMs used for NR were composed of 5 layer pairs of PDADMA/d-PSS separated by 4.5 layer pairs of undeuterated material. NR curves were recorded at different times during salt annealing. The Bragg peak in the NR curve due to the deuterated layer decreased in intensity with diffusion of d-PSS. The concentration of d-PSS was estimated from the scattering length density (SLD) profile. The diffusion coefficient ($D_{\perp} \sim 2 - 6 \times 10^{-17}$ cm^2/sec) was then estimated by studying the concentration of d-PSS at the peak as a function of time.

As mentioned before, Xu *et al.* concluded that diffusion in PEMs is anisotropic.[57] The perpendicular diffusion coefficient in this case was measured using NR. In the PEMs used for NR, every fifth bilayer of polycation/polyanion was composed of deuterated PMAA. The diffusion coefficient was estimated from the change in roughness of deuterated layer as:

$$\Delta\sigma_{int}^2 = 2D_{\perp}\Delta t \qquad (5)$$

where $\Delta\sigma_{int}$ is change in interfacial roughness, Δt is the salt annealing time, and $D_{\perp}$ is the diffusion in perpendicular direction. $D_{\perp}$ increased with increase in concentration of annealing salt solution.

In comparing diffusion studies by FRAP and NR, it becomes clear that the two techniques are limited in that they can only access parallel or perpendicular directions, respectively. Further, both techniques require labelling of some sort, which may require complex synthesis or may indirectly affect the actual diffusion of the polymer chains.

3.4 Quartz crystal microbalance with dissipation

QCM-D monitors *in situ* changes in the hydrated mass of a PEM, which offers the opportunity to measure chain diffusion into the PEM from an external solution. Specifically, Zan *et al.* estimated the diffusion coefficient of PSS in PSS/PDADMA PEMs.[64] PEMs built at 0.5 M NaCl were exposed post-assembly to various salt concentrations (0.75 – 2.5 M) until equilibrium was reached. Then, the PEMs were exposed to PSS with identical salt concentration, and the change in frequency was monitored as a function of time. The initial slope of q vs t, where q is given by Equation 6, allowed for the calculation of the diffusion coefficient of PSS using Equation 7.

$$q = \frac{\Delta f_0 - \Delta f}{\Delta f_0 - \Delta f_\infty} \quad (6)$$

$$D = \frac{\pi H^2}{4}\left(\frac{q}{t^{\frac{1}{2}}}\right)^2_{t \to 0} \quad (7)$$

where Δf_0 is the initial value, Δf_∞ is the steady state value, Δf corresponds to frequency at time t, and H is the initial PEM thickness. It was found that *D* increased dramatically from 5.5×10^{-14} to 1.6×10^{-12} cm²/sec when salt concentration increased from 1.0 to 1.5 M.

Zan *et al.* also investigated whether the diffusion of PSS adsorbing in the PEM was Fickian or not.[64] A reasonable superposition was obtained for various salt concentrations with the theoretical curve. Additionally, the authors[64] found a better fit for the uptake kinetics using a biexponential model, but did not use it further because it had three adjustable parameters (two exponential time constants and a factor with no physical significance). As suggested by Guzman *et al.* the presence of fast and slow times in the biexponential model may be related to the adsorption of polyelectrolyte at surface and reorganization of polyelectrolyte within the PEMs.[70]

3.5 Radiolabelling and Fourier transform infrared spectroscopy

As an alternative to labelling the polymer itself, as one might do for FRAP or NR, radiolabelled small counterions may be used to monitor the exchange or formation of extrinsic ion pairs. This allows for the determination of site diffusion in the PEM.

Specifically, Fares *et al.* studied adsorption of PDADMA and/or PSS chains into PDADMA/PSS PEMs using radiolabelling and FTIR spectroscopy.[66] PEMs overcompensated with either the polycation or the polyanion were immersed in NaCl solution containing radiolabelled species ($^{22}Na^+$ or $^{35}SO_4^{2-}$). The amount of radiolabelled species measured with a scintillator was an indication of number of extrinsic sites in the overcompensated PEMs. The PSS and PDADMA uptake kinetics were studied by monitoring the number of extrinsic sites with time. The diffusion coefficient of both PDADMA and PSS scaled exponentially with salt concentration, and at 1 M Na Cl, their values were 5.9×10^{-13} vs 4.4×10^{-14} cm²/sec, respectively), which was orders of magnitude higher than that obtained using FTIR spectroscopy.

This brings an interesting view in that the observed "diffusion" may be attributed to the PE chain, its sites, or its counterions, depending on the method of observation. Fares *et al.*[66] suggested that in the case of FTIR spectroscopy, 'polymer-dominated' diffusion is observed, wherein the polyelectrolyte molecule traverses the entire PEM by reptation. In contrast, 'site-dominated' diffusion is observed in radiolabelling, wherein the added polyelectrolyte is incorporated on the PEM surface through the conversion of intrinsic ion pairs into extrinsic ion pairs, in which these extrinsic sites propagate throughout the entire PEM. Thus, diffusion coefficients measured in the case of 'site-dominated' diffusion corresponded to diffusion of extrinsic ion pairs within the PEM, which is much faster than PE diffusion. Based on the magnitude of the diffusion coefficients the authors further suggested that QCM-D[64] monitors 'site-dominated' diffusion, and that NR monitors 'polymer-dominated' diffusion.[59]

4. Rheological behaviour for solid- and liquid-like polyelectrolyte complexes

The phase behaviour and single-chain polyelectrolyte dynamics ultimately influences the bulk mechanical properties and relaxation times in PECs and PEMs. First, we compare the mechanical behaviour for solid complexes and coacervates, in which we discuss three different relaxation times observed in the viscoelastic spectra of PECs. Next, sticky Rouse and sticky reptation models used to describe the mechanical behaviour of PECs are presented. Finally, relations among time, temperature, salt and pH are presented with a focus upon superposition principles.[30, 71, 72]

4.1 Solid- vs liquid-like rheological measurements of polyelectrolyte complexes in practice

Dynamic mechanical rheological experiments provide insight into various relaxation modes exhibited by polyelectrolyte complexes, allowing one to understand the dynamics of ion pair (re)formation, relaxation of chains between entanglements, and long-term relaxations. Depending on whether the complex is liquid- or solid-like, rheometery or dynamic mechanical analysis is appropriate. For coacervates, rheometers using cone and plate,[73] parallel plate,[51] or annular Couette cell[74] geometries have been used. For solid-like precipitates, rheometers using a parallel plate geometry[51] have been used. In addition, solid PEC precipitates processed into films[30] and fibers[75] were examined using dynamic mechanical analysis in tension mode, which is not possible for coacervates.

4.2 Relaxation times in polyelectrolyte complexes

Recent work has revealed the presence of several relaxation times that capture various dynamic processes occurring within the PEC. Yang *et al.* observed four distinct regions of behaviour for coacervates, [71] assigned to terminal, rubbery plateau, transition and glassy regions. In addition, the authors observed three crossover points in the viscoelastic spectra, corresponding to the following relaxation phenomena:

1. Relaxation at high frequencies (glassy to transition region), represented by the time for an intrinsic ion pair to (re)form,
2. Relaxation at intermediate frequencies, attributed to the relaxation of polyelectrolyte chains between entanglements, and
3. Relaxation at low frequencies, assigned to the long-range motion of chains.

Recently, Akkaoui *et al.* attributed the crossover at high frequencies to exchange between two pairs of intrinsic ion pairs (quadrupolar pair exchange).[76] This was supported by the fact that the activation energy of quadrupolar pair exchange estimated from rheological measurements was close to twice the activation energy of the hopping of a counterion. The long-range relaxation of

polyelectrolytes within a PEC has been described using both sticky Rouse and sticky reptation models, **Figure 2**.

Even though Yang *et al.*[71] were able to observe four distinct regions in the viscoelastic spectrum, the behaviour in glassy region was not well described, likely because coacervates were explored instead of solid-like precipitates. The glassy rheological behaviour of solid-like PECs has been described for saloplastics and solid films.[30, 77] In our own work, we performed dynamic mechanical measurements on solid PEC films and observed glassy behaviour ($G' > G''$), at various relative humidities;[30] time-water superposition (TWSP) was applied, and a very long relaxation time of 10^8 s was observed, which was attributed to the relaxation time of intrinsic ion pairs. It is likely that this relaxation time was very long because of the low hydration of the PEC.

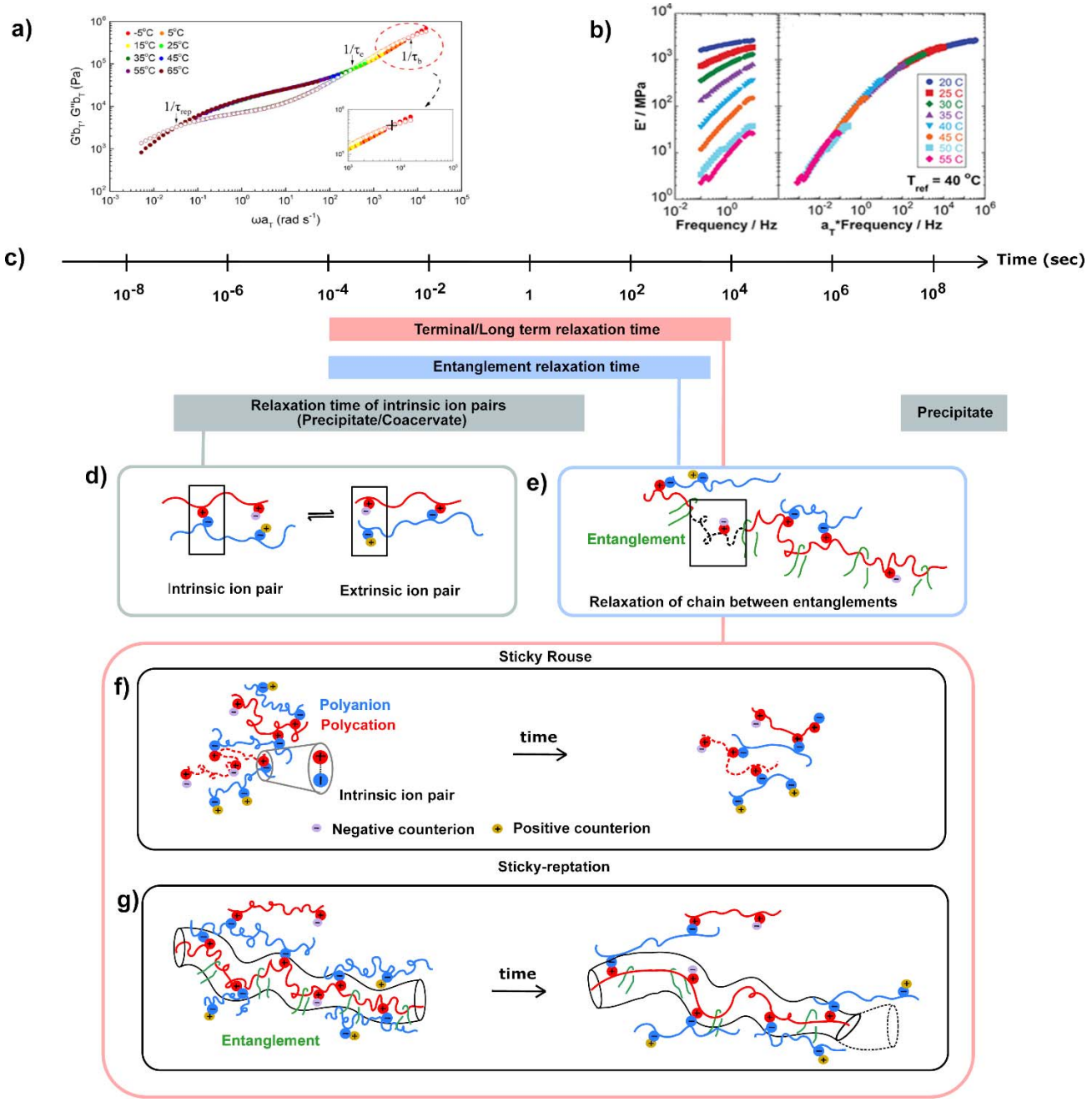

Figure 2: (a) Time-temperature superposition of coacervate indicating relaxation of intrinsic ion pairs, τ_b (τ_s); entanglement time (onset), τ_e; reptation time, τ_{rep}. Reprinted (adapted) with permission from ref. [65]. Copyright 2019 American Chemical Society. (b) Left panel shows storage modulus at 90 % RH for PAH/PAA solid precipitates over a temperature range of 20–55 °C. Right panel shows time-temperature superposition master curve. Legend in right panel applies to all panels in (b). Reprinted (adapted) with permission from ref. [29]. Copyright 2019 American Chemical Society. (c) Time scales for terminal relaxation time, entanglement relaxation time, and relaxation of intrinsic ion pair in precipitates and coacervates. (d) Schematic representation of intrinsic to extrinsic ion pair relaxation. (e) Schematic representation of chain relaxation between entanglements, which is represented by the dotted segment. (f) Schematic representation of a PEC composed of short chains, which relax via a sticky Rouse mechanism. (g) Schematic representation of a PEC composed of long chains, which relax by a sticky-reptation mechanism. The chain "reptates" inside the tube (shown by the black solid line).

4.3 Rouse and sticky Rouse models

The sticky Rouse model has been invoked to describe the behaviour of PECs, for the case of unentangled chains.[69, 78, 79] We first refresh the reader on the Rouse model, and then we discuss the sticky Rouse model as it is applied to PECs.

The Rouse model is used to describe dynamics of unentangled polymer melts.[80] A polymer chain is approximated as a sequence of N beads connected by N-1 springs. Each bead has a friction coefficient, ζ and each spring is composed of several monomer units with a root mean square (rms) length, b.[81] The Rouse time is expressed as follows[82]:

$$\tau_R \approx \tau_0 N^2 \qquad (8)$$

where τ_0 is the relaxation time for an individual bead. The relaxation modulus at $t = \tau_p$, $G(\tau_p)$, is the product of thermal energy k_BT and number density of sections with (N/p) monomers. Thus, $G(\tau_R)$ is:

$$G(\tau_p) = k_BT\frac{\varphi_p p}{Nb^3};\ G(\tau_R) = k_BT\frac{\varphi_p}{Nb^3} \qquad (9)$$

where G is the modulus, φ_p is the polymer volume fraction, T is the temperature and k_B is Boltzmann's constant. Finally, the zero shear viscosity for the Rouse model is described as:

$$\eta_0 = \int_0^\infty G(t)dt \approx \frac{\zeta\varphi_p}{b}N \approx G(\tau_R)\tau_R \qquad (10)$$

Thus, for unentangled polymer chains the Rouse model predicts $\eta_0 \sim N$.

However, in the case of PECs, the Rouse model is not applicable because the lifetimes of polymer interchain interactions are close to the thermal energy at room temperature. Thus, the breaking and reformation of these weaker interchain polymer interactions enter the timescale of experimental observation and become reversible.[83, 84] Rubenstein and Semenov developed the sticky Rouse model to describe the dynamics of unentangled solutions of associative polymers.[85] In the case of PECs, the intrinsic ion pairs control relaxation over long time scales and facilitate stress relaxation. The breaking and reformation of intrinsic ion pairs is considered an activated process. The timescale for intrinsic ion pairs breaking and reforming is known as the association lifetime, τ_s. At timescales <τ_s, the intrinsic ion pair behaves as a cross link.

We first examine the sticky Rouse model as it applies to unentangled PECs. Consider a polymer chain with a number of Kuhn repeat units as N and f associations (sticky points). Therefore,

$$N = fl \qquad (11)$$

where l is number of repeat units in between two stickers, where the sticker is an intrinsic ion pair. These sticky points act as friction centers and increase the relaxation time. The sticky Rouse time for unentangled solutions of associative polymers, τ_{SR}, then becomes:

$$\tau_{SR} \approx \tau_s f^2 \approx \tau_s\frac{N^2}{l^2} \qquad (12)$$

Similar to the Rouse model, the sticky Rouse model viscosity is proportional to the product of Rouse time and relaxation modulus at the Rouse time:

$$\eta_0 \approx \tau_R\frac{kT}{Nb^3}\varphi_p \approx \tau_s\frac{kT}{b^3l^2}N\varphi_p \qquad (13)$$

Thus, for unentangled associative polymer chains, such as for a PEC, the sticky Rouse model predicts $\eta_0 \sim N$.

4.4 Reptation and sticky-reptation models

With increasing polymer chain length, the movement of the chain becomes restricted due to intermolecular entanglements. The effect of entanglements on the relaxation time is considered by the reptation model, for which the relaxation of a single flexible chain trapped in a tube of entanglements occurs through wiggling or reptation.[86] The entanglement time, τ_e, is the Rouse time for relaxation of a chain between entanglements and is given by[82]:

$$\tau_e \approx \tau_0 N_e^2 \qquad (14)$$

where N_e is the number of Kuhn monomer units in an entanglement. Thus, the time taken for a polymer to diffuse a distance of the order of its size is longer than τ_R and assigned as the reptation time, τ_{rep}[82]:

$$\tau_{rep} \approx \tau_e\left(\frac{N}{N_e}\right)^3 \approx \tau_0\frac{N^3}{N_e} \qquad (15)$$

Accordingly, viscosity scales as $\eta_0 \sim N^3$ for the reptation model, which deviates slightly from the experimental value of $\eta_0 \sim N^{3.4}$.

However, the dynamics of entangled solutions of associative polymers, such as for polyelectrolyte complexes, is better-described by the sticky-reptation model. The sticky-reptation model is effectively a sticky Rouse model in a tube.[87] The sticky-reptation time is defined as the product of the sticky Rouse time and the number of entanglements per chain. Thus,

$$\tau_{srep} \approx \tau_{SR}\frac{N}{N_e} \approx \tau_s\frac{N^3}{l^2N_e} \qquad (16)$$

The zero shear viscosity is product of relaxation modulus and reptation time:

$$\eta_0 \approx \tau_{srep}\frac{kT}{N_eb^3}\varphi_p \approx \tau_s\frac{kT}{b^3l^2}\frac{N^3}{{N_e}^2}\varphi_p \qquad (17)$$

Finally, the scalings for the longest relaxation time and zero shear viscosity with respect to degree of polymerization for various models are given in the **Table 1**.

4.5 Identification of sticky Rouse and sicky-reptation regimes for polyelectrolyte complexes

The defining difference between sticky Rouse and sticky reptation regimes is the point at which the polyelectrolyte chain

Table 1. Scaling for long-term relaxation time and viscosity with respect to the number of Kuhn repeat units for various models.

Model	$\tau_{longest}$	η_0
Rouse	N^2	N
Reptation	N^3	N^3
Sticky Rouse	N^2	N
Sticky-reptation	N^3	N^3

becomes entangled. A plot of long-term relaxation time or viscosity vs chain length may be used to identify whether the relaxation occurs within sticky Rouse or sticky-reptation regimes, **Figure 3**. In describing the polyelectrolyte complex, which consists of a polycation and a polyanion having degrees of polymerization of n_{cat} and n_{an}, respectively, it is convenient to use the average chain length, n_{avg}. This value is assumed to be arithmetic average of n_{cat} and n_{an}.

Yang *et al.* identified the transition from sticky Rouse to sticky-reptation by studying the viscosity of coacervates of different chain lengths ($n_{avg} = 213 - 2097$) and various salt concentrations (0.03 – 0.3 M NaCl).[71] For coacervates prepared at low salt concentrations (0.03 – 0.1 M), a scaling of $\eta_0 \sim N$ for $n_{avg} \leq 343$ and $\eta_0 \sim N^{3.4}$ for $n_{avg} > 343$ indicated that relaxation took place through sticky Rouse and sticky-reptation, respectively. From the viscoelastic data for $n_{avg} = 343$ at 0.03 M NaCl concentration, the storage modulus (G') and loss modulus (G'') touched but did not cross, which supported that this chain length demarcated the sticky Rouse and sticky-reptation regimes.

In a follow-up study,[76] Akkaoui *et al.* observed a scaling of $\eta_0 \sim N^5$ for coacervates well into the entanglement regime ($n_{avg} = 1070 - 4740$). The enhanced viscosity was due to the longer reptation times. The authors[76] suggested that relaxation was facilitated by correlated breaking and exchange between a pair of intrinsic ion pairs (*i.e.,* a quadrupole). Thus, the reptation time increased by a factor of $(f/N_e)^2$, which was related to the probability of breaking of pair of intrinsic ion pairs at a specific entanglement.

Hamad *et al.* identified the transition from sticky Rouse to sticky-reptation by evaluating the long term relaxation time for coacervates with varying molecular weights of polyanion ($M_w = 11$, 82, 196 and 410 kg/mol).[79] Coacervates prepared with the two lowest polyanion molecular weights relaxed through a sticky Rouse mode and those prepared with the highest polyanion molecular weight of relaxed through a sticky-reptation mode. The entanglement molecular weight, estimated as crossover between these two regimes, was found to be 100 kg/mol ($n_{an} = 463$). It is important to note that the linear charge density for the polyanion was twice that of the polycation.

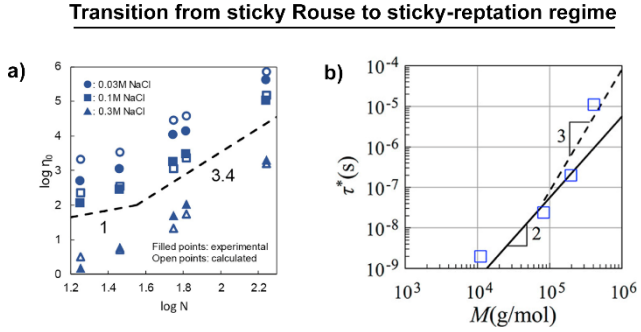

Figure 3: Transition from sticky Rouse to sticky-reptation regimes. (a) Zero shear viscosity of PECs at various salt concentrations (circle: 0.03 M, square: 0.1 M, triangle: 0.3 M NaCl) plotted against number of Kuhn segments (based on n_{avg}). Filled points are experimental values and open points are based on theoretical equations. The dashed line represents scaling of $\eta_0 \sim N$ and $\eta_0 \sim N^{3.4}$. Reprinted (adapted) with permission from ref. [65]. Copyright 2019 American Chemical Society. (b) Plot of $\tau^* = \tau_c \exp(-nE_a/k_BT)$ against polyanion molecular weight. The solid and dashed line represent scaling of $\tau^* \sim M^2$ and $\tau^* \sim M^3$ respectively. Open square represents experimental values obtained from rheological measurements. Reprinted (adapted) with permission from ref. [73]. Copyright 2018 American Chemical Society.

In contrast, Spruijt *et al.* studied the relaxation time of coacervates prepared with mismatched chain lengths, but similar linear charge densities. A decrease in polycation length lead to a decrease in relaxation time. In contrast to the results from Hamad *et al.*[79], no change in rheological response was observed with changing the polyanion length.[88] The polyanion length impacted the viscoelastic properties only when the polyanion chains were significantly longer than the polycation chains. The possible reasons for these two different conclusions may be that one study used matched linear charge densities, whereas the other study used mismatched, or else the different polyelectrolyte species studied.

In a separate study by Spruijt *et al.,* the terminal relaxation time for coacervates composed of PDMAEMA and PAA had a power-law slope of 2 ± 0.3 with respect to N (n_{avg}) at 0.6 M NaCl.[88] Thus, relaxation in these coacervates ($n_{avg} = 19 - 1128$) was successfully described by the sticky Rouse model. However, there was a deviation in the scaling of viscosity predicted by sticky Rouse model. A scaling of $\eta_0 \sim N^{2.3}$ at low salt concentration and $\eta_0 \sim N^{1.2}$ at high salt concentration was reported.[88] The sticky Rouse model was derived with the assumptions that distance between stickers and volume fraction of polymer was independent of chain length.[87] The authors suggested that these assumptions do not always hold for coacervates.[88] Specifically, φ_p also varies with salt concentration.[49] Thus, the power law dependence of η_0 with N should be evaluated keeping in mind the dependence of φ_p on N and salt concentration.

4.6 Time-temperature superpositioning of polyelectrolyte complexes

As viscoelastic materials, PECs exhibit dynamic properties that are dependent on both time and temperature. When both affect the PEC dynamics in a similar physical manner, their response may be superimposed using the time-temperature superposition principle (TTSP). To perform TTSP, frequency sweep data obtained at different temperatures are shifted along the frequency axis using a horizontal shift factor, a_T, which represents the ratio of relaxation time at temperature (T), τ_T, and at reference temperature (T_{ref}), $\tau_{T_{ref}}$[81]:

$$a_T = \frac{\tau_T}{\tau_{T_{ref}}} \qquad (18)$$

Given whether the PEC is a solid, a liquid, or its proximity to the T_g, TTSP generally may be captured using one of two models: Arrhenius or Williams-Landel-Ferry (WLF). For solid PECs, the horizontal shift factors have been fit to both the Arrhenius and WLF equations. In the case of coacervates, the horizontal shift factor is usually fit to the WLF equation, but the use of the Arrhenius equation has also been reported. **Table 2** summarizes the application of these and other models. These are elaborated below in consideration of increasing temperature in proximity of the T_g.

Table 2: Horizontal and vertical shift factors used to perform time-temperature superposition in solid polyelectrolyte complexes and liquid-like coacervates

Polycation	Polyanion	Precipitates or Coacervates	Equation used to fit Horizontal shift factor, a_T	Vertical shift factor, b_T	Reference
Poly(allylamine hydrochloride)	Poly(acrylic acid)	Solid precipitate	Arrhenius	Not used	[30]
Poly(diallyldimethylammonium chloride)	Poly(4-styrenesulfonic acid, sodium salt)	Solid precipitates	WLF	Not used	[77]
Poly(diallyldimethylammonium chloride)	Poly(4-styrenesulfonic acid, sodium salt)	Solid precipitate and Coacervates	WLF	Not used	[78]
Quaternized poly(4-vinylpyridines)	Poly(4-styrenesulfonic acid, sodium salt)	Coacervates	Vogel–Fulcher–Tammann form of WLF	Not used	[73]
Poly[3-(methacryloylamino)propyltrimethylammonium chloride]	Poly(sodium methacrylate)	Coacervates	Arrhenius	Used	[76]

When $T < T_g$ the Arrhenius equation has most successfully described a_T.[89] For example, we applied TTSP for solid PAA/PAH complexes at different RH (50 – 95 %).[30] For low RH values (50-85 %), the studied temperatures were below and near the T_g, and the horizontal shift factors were well-described by the Arrhenius equation:[30]

$$\ln(a_T) = \frac{E_a}{R}\left(\frac{1}{T} - \frac{1}{T_{ref}}\right) \qquad (19)$$

where E_a represents the activation energy required to break an intrinsic ion pair. It is also noted that the Arrhenius equation may be used when the temperature range is small.

When $T > T_g$ the WLF equation has most successfully described a_T, so long as $T > T_g + 100\ ^0$C.[89] The WLF equation is given by:

$$\log(a_T) = \frac{-C_1(T-T_{ref})}{C_2+(T-T_{ref})} \qquad (20)$$

where C_1 and C_2 are adjustable parameters. For solid PECs, we reported reasonable parameter values when a_T was described by the WLF equation only for specimens equilibrated at high RH (90,95 %), when T>T_g.[30] Shamoun *et al.* performed TTSP using the WLF equation for extruded saloplastics at various salt concentrations and temperatures;[77] the C_1 and C_2 values were within expected values for WLF theory.[81] These prior two examples show that solid PECs may be described using WLF theory when there is a high water content, when T>T_g, and/or when salt concentration is high.

In contrast to solid PECs, liquid-like coacervates have higher water content. Hence, coacervates may have a very low T_g (if any). Thus, the WLF equation is most often used to describe a_T for coacervates.[73, 78] For example, TTSP for PSS/PDADMA coacervates at various salt concentrations was applied using the WLF equation without the need for vertical shift factor. [78]

Sadman *et al.* performed TTSP for coacervates and used an equivalent form of WLF equation known as the Vogel-Fulcher-Tammann (VFT) equation.[73] The horizontal shift factor with B and T_∞ as the parameters is given by:

$$\log(a_T) = \frac{-B}{T_{ref}-T_\infty} + \frac{B}{T-T_\infty};\ B = C_1C_2\ ;\ C_2 = T_{ref} - T_\infty \qquad (21)$$

When $T > T_g + 100\ ^0$C the Arrhenius equation may described a_T.[89] Akkaoui *et al.* performed TTSP on coacervates using Arrhenius behavior;[76] in this case, E_a represented the activation energy for exchange between two intrinsic ion pairs. Although the T_g was not reported, we believe that the measurements taken by Akkaoui *et al.* may have proceed far above the T_g

Many of the preceding reports have invoked the use of a vertical shift factor, b_T, to facilitate in superimposing rheological data. Sometimes, the vertical shift is performed arbitrarily without physical explanation, and, in other cases, the vertical shift is explained as changes in sample density with temperature:

$$b_T = \frac{\rho_{ref}T_{ref}}{T\rho} \qquad (22)$$

where ρ is sample density at temperature T and ρ_{ref} is sample density at T_{ref}. Thermorheologically simple materials do not need a vertical shift factor to perform TTSP.[90] In contrast, thermorheologically complex materials may require a vertical shift factor. The need for a vertical shift factor can be observed using a van Gurp-Palmen plot in which loss angle is plotted against $\log|G^*|$, where G^* is the complex modulus.

Besides superpositioning of rheological information, TTSP has also been applied to describe conductivity spectra of dried and hydrated PECs.[91, 92] When TTSP holds true for conductivity spectra, the mechanism of ion transport does not change with temperature, and dynamics on all time scales will be equally accelerated with increasing temperature.[92]

Imre *et al.* analyzed the conductivity spectra of dried PSS-PDADMA complexes at different temperatures and composition (35 mole % to 70 mol % PSS).[91] At constant temperature, the dc conductivity increased with increasing PSS content and thus conductivity was dominated by Na^+ ions. To perform TTSP, the authors used a rescaling parameter in the frequency domain (ϑ_0):

$$\vartheta_0 \propto \sigma_{dc}TT^{-\alpha} \qquad (23)$$

where σ_{dc} is the dc conductivity. The parameter α was allowed to vary, and a value of $\alpha = 0$ indicates Summerfield scaling. For PECs rich in PSS, TTSP was successful at all measured frequencies and temperatures, whereas there was a slight deviation observed at very high normalized frequencies for PECs rich in PDADMA.

De *et al.* applied TTSP to temperature-dependent conductivity spectra of hydrated PSS-PDADMA PECs.[92] The RH was varied from 30 to 80 %, and Summerfield scaling was successfully applied to perform TTSP. The applicability of Summerfield scaling suggested that: 1) the number density of mobile ions did not change with temperature, 2) the number of available ion sites did not change with temperature, and 3) the ion mobility increased with temperature.

4.7 Time-salt superpositioning of polyelectrolyte complexes

The doping of PEMs with salt leads to conversion of intrinsic ion pairs to extrinsic ion pairs thus decreasing the number of intrinsic ion pairs and enhancing the movement of polyelectrolyte chains within the PEM.[57] This phenomenon draws comparison with the accelerating effects of temperature and time in PECs. At t < τ_s, the intrinsic ion pair behaves as a crosslink and at t>τ_s, the relaxation is controlled by the amount of intrinsic ion pairs (salt) and the association lifetime. The equivalency between time, temperature, and salt can be captured by time-salt superposition (TSSP) and time-temperature salt superposition (TTSSP) principles. For example, to perform TSSP, a series of frequency sweeps at different salt concentrations are converted to a master curve by performing rescaling in frequency and modulus scales. The horizontal shift factor, a_s, represents changes in relaxation time with salt concentration (c_{salt}).

TSSP and TTSSP have been performed for both solid PECs and liquid-like coacervates. In the case of solid PECs, the effect of c_{salt} on a_s has been captured by an empirical relationship.[77] In the case of liquid-like coacervates, the relationship between c_{salt} and a_s is captured by the sticky Rouse model, which results in a stretched exponential scaling for a_s with respect to c_{salt}.[69] Additionally, an exponential scaling has also been used.[73] **Table 3** summarizes these and other scalings for a_s. First, we will discuss the application of TSSP and TTSSP to solid PECs and scaling used for a_s. Next, we will examine salt-superpositioning across the precipitate-coacervate continuum. Lastly, we discuss the application of TSSP and TTSSP to coacervates and various scaling used to describe a_s.

Shamoun *et al.* performed TTSSP for extruded saloplastics by shifting TTSP curves of complex modulus (G^*) obtained at different salt concentrations.[77] The scaling for a_s with respect to c_{salt} was given by: $a_s \sim \exp\left(-[c_{salt}]^{\frac{6}{5}}\right)$.

Table 3 Horizontal and vertical shift factors used to perform salt superpositioning in solid polyelectrolyte complexes and liquid-like coacervates

Polycation	Polyanion	Scaling for horizontal shift factor, a_s, with salt concentration, c_{salt}	Vertical shift factor	Reference
Poly(diallyldimethylammonium chloride)	Poly(4-styrenesulfonic acid, sodium salt)	$\sim\exp\left(-[c_{salt}]^{\frac{6}{5}}\right)$	Not used	[77]
Poly(diallyldimethylammonium chloride)	Poly(4-styrenesulfonic acid, sodium salt)		Used	[51]
Poly(diallyldimethylammonium chloride)	Poly(4-styrenesulfonic acid, sodium salt)	$\sim\exp\left(-\sqrt{c_{salt}}\right)$	Used	[78]
Poly(N,N-dimethylaminoethyl methacrylate)	Poly(acrylic acid)	$\sim\exp\left(-\sqrt{c_{salt}}\right)$	Used	[69]
Poly(N,N-dimethylaminoethyl methacrylate)	Poly(acrylic acid)	$\sim\exp\left(-\sqrt{c_{salt}}\right)$	Used	[88]
Poly(diallyldimethylammonium chloride)	poly(isobutylene-alt-maleate sodium)	$\sim\exp\left(-n\sqrt{c_{salt}}\right)$	Used	[79]
Poly(L-lysine hydrochloride)	poly(D,L-glutamic acid sodium salt)	$\sim\exp(-c_{salt})$	Not used	[93]
Poly(diallyldimethylammonium chloride)	quaternized poly(4-vinylpyridines)	$\sim\exp(-c_{salt})$	Not used	[73]
Poly[3-(methacryloylamino)propyltrimethylammonium chloride]	Poly(sodium methacrylate)	$a_{s,\tau_b}a_{s,f}a_{s,\varphi}$	Used	[71]
Poly[3-(methacryloylamino)propyltrimethylammonium chloride]	Poly(sodium methacrylate)	$a_{s,\tau_b}a_{s,f}a_{s,\varphi}a_{s,N_e}a_{s,d}$	Used	[71]
Poly(ethyleneimine)	Poly(D,L-glutamic acid) (PGlu)		Used	[94]

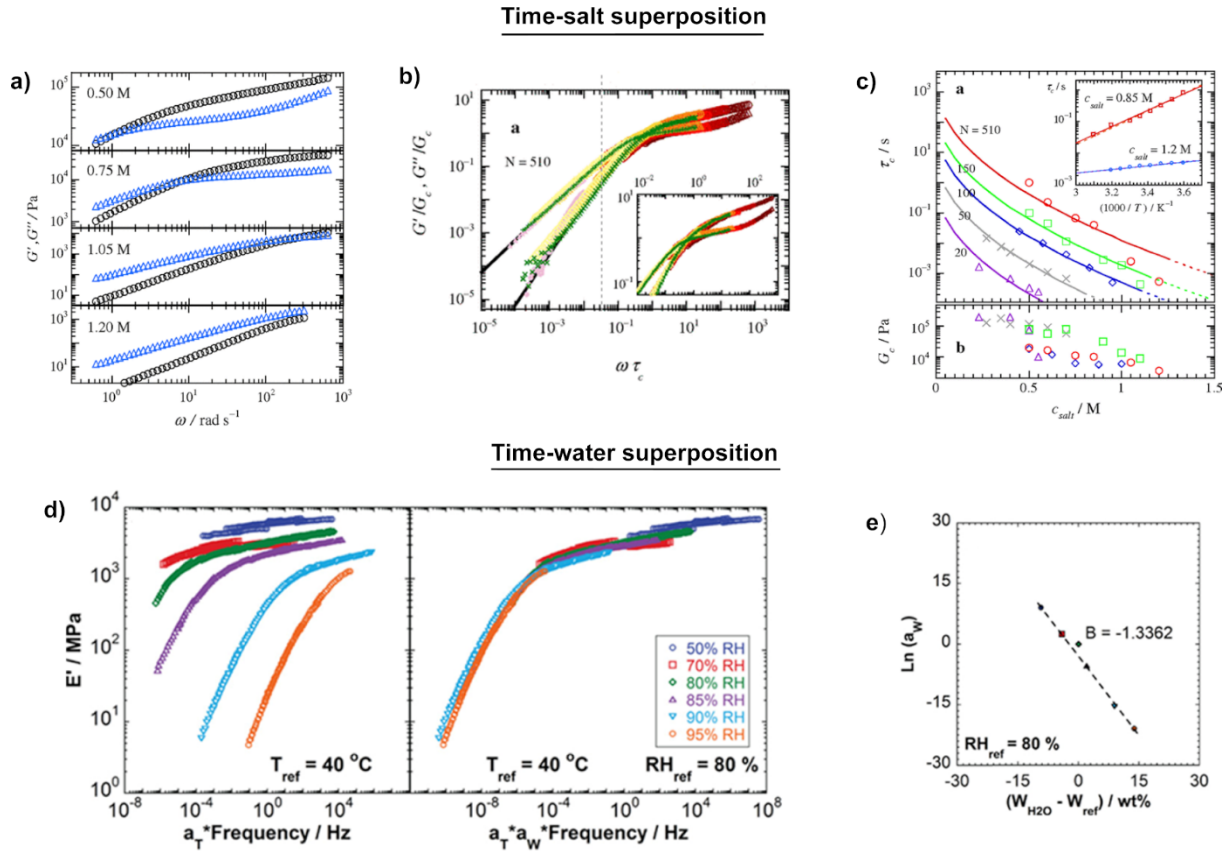

Figure 3: Frequency sweeps for polyelectrolyte coacervate at different salt concentrations (indicated in the figure). Circle and triangle represent storage and loss modulus respectively. (b) Master curves after performing time-salt superposition. Storage modulus is shown using circle and crosses. Loss modulus is shown using triangle and pluses. Filled symbols are data converted from creep testing. Solid lines are to guide the eye. (c) Relaxation times (horizontal shift factor) against salt concentrations at different average chain lengths (n_{avg}) indicated in the figure. The inset shows relaxation times at different temperatures at 0.85 M and 1.2 M NaCl. Solid and dashed line represents scaling of relaxation time to $\exp(T^{-1})$ and $\exp(T^{-1.5})$. Vertical shift factor against salt concentrations at different average chain lengths (n_{avg}). Legend in top panel applies to the bottom panel. (a-c) Reprinted from ref. [63]. (d) Time-temperature superposition curves at different RH. Right panel represents master curve obtained after performing time-water superposition to the data shown in left panel. (e) Water-dependent shift factor as a function of water content ($W_{H_2O} - W_{ref}$) in PECs. Dashed line represents fit to Equation 29. (d-e) Reprinted with permission from ref. [29]. Copyright 2019 American Chemical Society.

Liu *et al.* attempted TSSP across the precipitate-coacervate continuum.[51] The divergence observed in a Winter plot ($\eta^* \; vs \; G^*$), where η^* is complex viscosity, at intermediate salt concentration suggested that TSSP cannot be applied entirely across the precipitate-coacervate continuum. Hence, TSSP was performed separately for precipitates and coacervates. The authors did not discuss the scaling obtained for a_s. Ali and Prabhu also attempted TTSSP in the precipitate coacervate continuum.[78] The authors obtained a stretched exponential scaling for a_s, discussed later. The range of frequency over which the viscoelastic moduli, G' and G'', overlay into a master curve decreased with decreasing salt concentration. The above two studies[51, 78] suggest that it may not be possible to apply salt superposition across the precipitate-coacervate continuum.

Sprujit *et al.* demonstrated TSSP for coacervates prepared at different NaCl concentrations.[69] The response was solid-like at low salt concentration, 0.5 M NaCl ($G' > G''$), and liquid-like at high salt concentration, 1.2 M NaCl ($G'' > G'$). The relaxation of chains was discussed using a sticky dynamics model proposed by Rubinstein.[87] The intrinsic ion pairs acted as friction centers (sticky points) and the relaxation time was given by:

$$\tau_c \approx N^{\alpha} \varphi_p^{\beta} \zeta_0(c_{salt}) \qquad (24)$$

where τ_c is the long term relaxation time and ζ_0 is the effective friction coefficient. Salt facilitates the conversion of intrinsic ion pairs to extrinsic ion pairs and hence ζ_0 depends on c_{salt}. The activation energy, E_a, for breaking and reforming an intrinsic ion pair was estimated as the difference between the electrical energy of four separated ionic groups in a salt solution (obtained by Debye–Hückel equation) and columbic energy of two ions (*i.e.* one intrinsic ion pair) in contact:

$$\tau_s = \tau_0 \exp\left(\frac{E_a}{k_B T}\right) = \tau_0 \exp\left[-2kl_B + \frac{2l_B}{d}\right] \qquad (25)$$

where τ_0 is the attempt time,[79] l_B is the Bjerrum length, d is distance between two ions in an intrinsic ion pair, and k is the inverse Debye length (with $k \propto \sqrt{c_{salt}}$). Thus, τ_c was given by:

$$\tau_c \propto A \exp\left(-2a(T)\sqrt{c_{salt}}\right) \qquad (26)$$

where A was an adjustable prefactor. The variations in φ_p with c_{salt} were said to be small in comparison to that of τ_c with c_{salt}, and thus the effect of φ_p on the dynamics were neglected. Finally, the scaling for the horizontal shift factor was $a_{salt} \sim \exp\left(-\sqrt{c_{salt}}\right)$.

Ali and Prabhu performed TTSSP on solid PECs and liquid-like coacervates and used Equation 24 to describe a_s.[78] Also, the authors considered the effect of φ_p on relaxation times with a value of β as 7/3.

Hamad *et al.* performed TSSP on coacervates and modified the sticky dynamics treatment by assuming that multiple intrinsic ion pairs should break at once to allow large-scale motion.[79] Therefore,

$$\tau_c \propto A\exp\left(-na(T)\sqrt{c_{salt}}\right) \quad (27)$$

where n is the number of intrinsic ion pairs. Interestingly, the value of n (n=5) was the same for coacervates prepared with different chain lengths of polyanion. The effect of φ_p on relaxation time was not considered.

In contrast to the stretched exponential scaling of a_s with c_{salt} predicted by the sticky dynamics model, exponential scaling has also been used.[73, 93] Marciel *et al.* performed TSSP and a_s was described as $\varphi_p\exp(-c_{salt})$, but they were unsuccessful in fitting it to the relationship proposed by Sprujit *et al. i.e.* $a_s \sim \exp\left(-\sqrt{c_{salt}}\right)$.[93] The difference in hydrophobicity of polymer backbone and range of salt concentration explored was cited as the reason for the disagreement. In addition, the authors[93] considered the variation of φ_p on a_s. Sadman *et al.* also observed a_s scaled exponentially with c_{salt} (*i.e.*, $a_s \sim \exp(-c_{salt})$).[73]

The effect of φ_p on a_s has been unclear so far in the stretched exponential and exponential models. Recently, Dompé *et al.* found that relaxation times are dependent on polymer weight fraction in coacervates prepared from graft copolymers.[95] Yang *et al.* performed TTSSP and considered the effect of φ_p on relaxation times.[71] The authors postulated that increasing salt concentration impacts coacervate dynamics in three different ways: 1) a_{s,τ_b}, decreasing intrinsic ion pair lifetime, 2) $a_{s,f}$, decreasing the number of intrinsic ion pairs per chain, and 3) $a_{s,f}$, decreasing the polymer volume fraction.[71] Thus the overall the salt shift factor was:

$$a_s = a_{s,\tau_b}a_{s,f}a_{s,\varphi} \quad (28)$$

Recently, Akkaoui *et al.*[76] extended the previous work by Yang *et al.*[71] and considered the effect of change in N_e (a_{s,N_e}) and change in distance between a pair of intrinsic ion pairs ($a_{s,d}$) due to salt concentration in the overall salt shift factor used to perform TTSSP. This work highlights the need to consider the variation in N_e when studying relaxation times in coacervates in the entanglement regime.

In addition to the horizontal shift factor, various studies discussed so far have also employed vertical shift factors (b_s) to perform TSSP and TTSSP. The physical reasoning behind the application of b_s remains unclear. Liu *et al.* suggested that b_s accounts for correction in moduli caused by changes in φ_p with c_{salt},[51] but the authors do not discuss the opposite trend in b_s for precipitates and coacervates with respect to c_{salt}. Hamad *et al.* suggested that b_s reflected the number density of network strands.[79]

These studies have revealed the general role of salt in the dynamics of PECs, but they have so far neglected the complex role of water. As discussed next there are different microenvironments of water in hydrated PECs and PEMs,[96-98] and solid- and liquid-like PECs have very different degrees of hydration. These differences may be one of the reasons for failure of salt-superpositioning to completely capture the entire precipitate-coacervate continuum. Also related to water content, it will be important to consider the impact of water on φ_p when performing TSSP and TTSSP.

4.8 Time-water superpositioning of polyelectrolyte complexes

Dry PECs are glassy and brittle due to the large number of ion pair crosslinks. However, for hydrated PECs water acts as plasticizer, increases free volume, and facilitates the transition from a glassy to a rubbery state.[17] For example, Hariri *et al.* found that there was a strong nonlinear increase in tensile modulus of macroporous PECs with decreasing water content. Also, Huang *et al.* observed a glassy to rubbery transition in the tensile modulus of PEC fibers of alginate (ALG) and PDADMA due to increasing water content with relative humidity (RH).[75] The authors suggested that at low hydration the water molecules interacted more strongly with the intrinsic and extrinsic ion pairs resulting in plastic behaviour. In contrast at higher hydration, water molecules were loosely interacting with the ion pairs, which increased free volume and facilitated the transition to a rubbery state.

As with salt, water can also affect dynamic mechanical properties comparable to time and temperature in the form of time water superpositioning (TWSP). We studied the dynamic mechanical properties of PAH/PAA complexes at different RH (50 – 95%).[30] To perform TWSP, TTSP master curves at different RH were shifted horizontally. The horizontal shift factor used in TWSP, a_W, represented changes in the relaxation time with water and was related to the water content in specimen, W_{H_2O}, by:

$$\ln(a_W) = B\left(W_{H_2O} - W_{ref}\right) + c \quad (29)$$

where W_{ref} is the reference water content. The negative value of B suggested that water lowered the activation energy of the relaxation process. From simulations, the average number of intrinsic ion pairs formed by a single PAH repeat unit did not vary with temperature (20 – 55 °C) and decreased slightly (~2.32 to ~2.00) with hydration (18.7 to 31.7 wt%). This suggested that there was little-to-no change in relaxation mechanism with temperature and hydration, and thus supported the validity of both TTSP and TWSP for PAH-PAA PECs. The log-linear relationship of a_W with water content in Equation 29 closely follows the TWSP performed by De *et al.* on humidity-dependent conductivity spectra of PSS-PDADMA complexes.[99]

4.9 Time-pH superpositioning of polyelectrolyte complexes and hydrophobic considerations

The relaxation in coacervates is controlled by the dynamics of intrinsic ion pairs. Therefore, the number of intrinsic ion pairs, which is subsequently controlled through changes in pH, becomes an important factor for PECs formed from weak polyelectrolytes.

Tekaat *et al.* studied the effect of pH on the dynamics of coacervates and demonstrated time-pH superpositioning.[72] The coacervates were prepared from PDADMA, a strong polyelectrolyte and PAA, a weak polyelectrolyte, at different pH values (5-10) and

salt concentrations (0-0.50 M). The shear moduli obtained at different pH values were shifted on the frequency and modulus scale. The horizontal shift factor decreased with increasing pH and, like the degree of dissociation of PAA, it reached a plateau at high pH values. The decay was more pronounced for coacervates prepared at higher salt concentrations. The vertical shift factor was attributed to the changing polymer density but was not discussed further. The success of time-pH superposition suggested that changing the polyanion charge density only influenced the timescale of relaxation dynamics of coacervates and not the mechanism. The decrease in chain dynamics with decreasing pH was a result of friction arising from uncharged hydrophobic segments of PAA at low pH.

Recently, Huang *et al.* studied the viscoelastic behaviour of coacervates prepared with varying hydrophobicity of nonionic comonomer.[100] The nonionic comonomers were either hydrophobic (amide) or hydrophilic (butyl). Coacervates were prepared by mixing polyelectrolytes with a similar fraction of charged and nonionic monomers. Two Rouse-like relaxation processes (fast and slow) were used to describe the viscoelastic behavior. Unsurprisingly, the fast relaxation time (τ_{fast}) decreased with a decrease in charge density, but it did not follow the expected scaling behaviour of a sticky-Rouse model ($\tau_{SR} \sim f^2$). Contrary to the study by Tekaat *et al.*, τ_{fast}, was insensitive to the change in hydrophobicity of the non-ionic comonomer because the association energy of two hydrated butyl chains (hydrophobic segments) was less than the thermal energy at room temperature. Thus, the hydrophobic interactions were said to be short lived and did not affect τ_{fast}. This shows that hydrophobic interactions may influence the rheology of PECs in certain cases.

5. The glass transition in solid polyelectrolyte complexes and multilayers

As with neutral polymers, solid PECs and PEMs undergo a glass transition as mechanical properties change from glassy to rubbery. For solid PECs and PEMs, however, this transition occurs generally when in a hydrated state.[17, 101-106] The glass transition has manifested as physical changes observed using calorimetry, QCM-D, rheology, light scattering, NMR spectroscopy, as well as simulations.[6, 20, 77, 101, 103, 107-109] Water content, salt concentration, pH, terminating layer each influence the T_g of PECs and PEMs. T_g is dependent on the flexibility and mobility of individual polymer chains, which is further influenced by the number of intrinsic ion pairs or "stickers". In contrast, coacervates do not exhibit a glass transition because they are heavily hydrated and plasticized.

5.1 Water, intrinsic ion pairing, and the glass transition

Early observations by Michaels *et al.*[17] discuss the importance of water in plasticizing PECs. We have observed this firsthand in both PECs and PEMs in our own work. Whereas PAA or PAH homopolymers individually exhibit T_g values of 128 °C and 223 °C, respectively, dry PAH/PAA PEMs show no T_g over the temperature range investigated using modulated differential scanning calorimetry (MDSC).[105] Similar observations have been made for both PAH/PAA and PDADMA/PSS PEMs using QCM-D monitoring.[107, 108] PDADMA homopolymer exhibits a T_g at 170 °C whereas no T_g was observed for dry PDADMA/PSS below the degradation temperature of 250 °C. Thus, the T_g of dry PEMs may actually exist at temperatures above the PEMs' degradation temperature. This was attributed to the tightly packed structure and limited polymer chain mobility as a result of numerous intrinsic ion pairs.[107]

With some critical amount of water added to the solid PEC or PEM, a T_g appears. Interestingly, this plasticizing behavior appears to be (so far) unique to water. For example, PECs exposed to various alcohols (1-propanol, n-butanol and ethylene glycol) did not exhibit a T_g.[102]

More specifically, the water content within a PEC influences the value of its T_g for which slight changes in water content can result in large changes in the T_g. By increasing the hydration level from 16 to 24.8 wt%, we observed a reduction in the glass transition temperature of PDADMA/PSS PECs from 72 – 42 °C.[6] The plasticizing

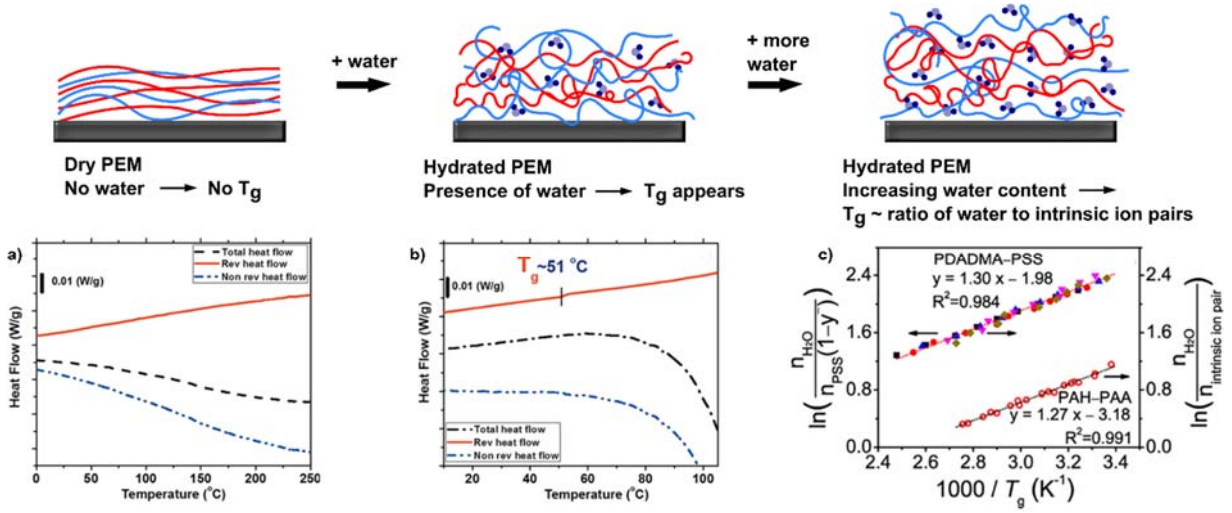

Figure 4: Relationship between water content of poly(diallyldimethyl ammonium chloride)/polystyrene sulfonate (PDADMA/PSS) polyelectrolyte multilayers and the glass transition temperature (T_g). MDSC thermographs of a) dry PEM and b) hydrated PEM reprinted with permission from ref. [102]. Copyright 2012 American Chemical Society. c) T_g-water relationship reprinted with permission from ref [20] Copyright 2018 American Chemical Society

effects of water have also been confirmed on PDADMA/PSS PEC fibers at different relative humidities by Lyu *et al.*[106] Using DMA, the PEC fibers had a T_g of 23.6 °C at 50 – 60 % RH and 59.5 °C at 10 %RH. Likewise, the T_g of PAH/PAA PECs determined using DMA or MDSC decreased with RH or water content, respectively.[30, 101] For DMA, T_g decreased from 72 to 35 °C as the RH increased from 70 to 85 %RH at pH 7.[30] For DSC, T_g decreased from 61 °C to 23 °C as water content increased from 15.3 to 24.2 wt % water at pH 3.5.[101] Water strongly influences the T_g because water plasticizes PECs and PEMs through hydrogen bonding.[101] Water within PECs and PEMs lubricates polymer chains while simultaneously weakening the ion pairs, which allows intrinsic ion pair exchange and segmental relaxation to more easily occur.

Salt is also an important factor governing chain relaxation and mobility and thus the T_g. Using MDSC, the effect of the ionic strength of mixing polyelectrolyte solutions has been studied.[20] This study showed that the glass transition temperature of PDADMA/PSS PECs at fixed hydration decreased as the preparatory salt content increased.[20] This study showed that the T_g of PDADMA/PSS PECs at fixed hydration decreased as the preparatory salt content increased. At 24 wt % water, T_g decreased from 72 – 32 °C (345 – 325 K) as salt concentration increased from 0 – 1.5 M NaCl. Thus, there was decrease in T_g due to doping by salt. This finding was confirmed elsewhere, in which Shamoun *et al.* presented a relationship between the T_g of extruded PDADMA/PSS PECs and NaCl concentration from DMA measurements.[77] The T_g was found to decrease with increase in salt concentration which was attributed to an increase in the fraction of extrinsic ion pairs. The effect of frequency (f) and salt concentration (c_{NaCl}) on T_g was described as:

$$T_g = 38 + 2.3\ln(f) - 20[c_{NaCl}]^{\frac{6}{5}} \qquad (30)$$

For the most part, salt acts as a plasticizer by breaking intrinsic ion pairs, but simulations suggest a special case in which salt works against plasticization.[6] For example, simulations suggest that at lower hydrations, salt ions tend to reduce the lubricating effect of water molecules by competing with intrinsic ion pairs for uptake into their hydration shells; thereby, this case would decrease the actual amount of water available for lubrication at the intrinsic ion pair.[6]

Specific to PEMs, the glass transition temperature can be influenced by the terminal layer,[29, 109, 110] for which surface charge and hydrophilicity of the terminal layer are factors. However, after thermal annealing, the T_g can became independent of the terminating layer.[109]

5.2 Simulations of the glass transition of polyelectrolyte complexes and multilayers

In addition to experimental studies, the glass transition has also been observed using simulations. By observing the bonds between water molecules and polyelectrolyte chains, MD simulations identified a transition temperature.[6, 20, 102] The number of water-PSS bonds per repeat unit in a PDADMA/PSS PEC generally decreased with increasing temperature but experienced a drastic decrease between 67 °C and 72 °C.[102] This discontinuity was considered as the thermal transition temperature. This transition was not observed for water-PDADMA bonds because PSS forms stronger hydrogen bonds than PDADMA.[102] This result was also confirmed in another simulation on PDADMA/PSS, which further shows that this loss of water-PSS hydrogen bonding is mainly from the intrinsic ion sites.[20] Another report[6] observed the T_g as a change in the water diffusion coefficient in PDAMA/PSS PECs.[20] Specifically, the diffusion coefficient increased with temperature, having different slopes below and above the T_g. Experimentally, changes in the water diffusion coefficient or water-PSS binding associated with the T_g have not yet been confirmed.

5.3 Correlations for the glass transition of polyelectrolyte complexes and multilayers

Given the multicomponent nature of PECs and PEMs, it is reasonable to first examine the possibility of using the Fox equation or other variants to describe the T_g. However, using the Fox equation alone is not applicable because of the highly ion-paired nature of the system. Instead, Fu *et al.* presented a modified Fox equation based on the doping level of the system.[103] The doping level of a PDADMA/PSS PEM was determined using ATR-FTIR spectroscopy as a function of temperature and salt. The T_g decreased as doping level increased. The T_g was partitioned into intrinsic and extrinsic contributions, T_{g_i} and $T_{g_{ex}}$, respectively and correlated to the intrinsic and extrinsic components (1-y and y, respectively) as:

$$\frac{1}{T_g} = \frac{1-y}{T_{g_i}} + \frac{y}{T_{g_{ex}}} \qquad (31)$$

As expected, $T_{g_{ex}}$ is of a much lower value than T_{g_i}. At high values of y = 0.4, a significant decrease in the value of $T_{g_{ex}}$ was observed, which was explained using the sticky reptation model. However, this model does not consider the effect hydration.

Given the strong influences of both water and salt on the T_g of PECs and PEMs, we have investigated their mutual influence, resulting in a correlation that has (so-far) proven applicable to both PECs and PEMs, as well as both strong and weak polyelectrolyte systems.[20, 101] Zhang *et al.* reported that the T_g is dependent on the ratio of number of water molecules to intrinsic ion pairs.[20] This dependence was verified for both weak (PAH/PAA) and strong (PDADMA/PSS) systems.[20] A linear relationship was obtained when ln(number of water molecules / number of intrinsic ion pairs) was plotted against $1/T_g$ as:

$$\frac{1}{T_g} \sim ln\left(\frac{n_{H_2O}}{n_{intrinsic\ ion\ pairs}}\right) \qquad (32)$$

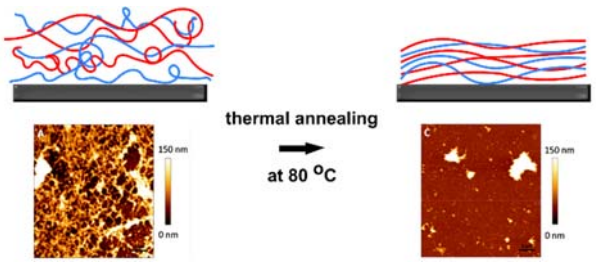

Figure 5: Effect of thermal annealing on the roughness of poly-l-lysine/alginate polyelectrolyte multilayer studied using atomic force microscopy. Reprinted from ref. [108] with permission from Elsevier

By linking Equation 32 to the van't Hoff relationship, an energy term (R × slope) was determined to be 10.6-10.8 kJ/mol for all systems studied thus far. The value of this energy term agrees with the van't Hoff enthalpy of the breaking of one hydrogen bond, 10.5 ± 2.5 kJ/mol. This suggests that the glass transition is mediated by the breaking and reformation of intrinsic ion pairs, facilitated by hydrogen bonding water in the hydration shell of the intrinsic ion pair.

5.4 Consequences of thermal annealing in polyelectrolyte multilayers

Post-assembly thermal treatment of both PECs and PEMs influences the structure, density, conformation, thickness, refractive index, diffusion, and water content.[96, 111] Thermal annealing above the T_g usually results in smoother PEMs and greater intermixing of the PEM layers.[112] Further, according to Equations 31 and 32, the annealing T_g may be further adjusted by changing the salt concentration of the annealing environment (thereby changing y).

For example, the effects of thermal annealing on PDADMA/PSS and PDADMA/PSS-PNIPAM films prepared at 0.5 M NaCl were studied using neutron reflectometry.[113] Both samples exhibited increased Kiessig fringes with increasing temperature to 60 °C, consistent with a decrease in roughness. Thermal annealing of PEM microcapsules has also resulted in plastic deformation, swelling, or expansion, depending on the terminal layer.[114, 115] Zerball *et al* described morphological changes occuring in outermost PEM layers while innermost layers became denser during thermal annealing.[111] They also showed that thermal treatments influence the swelling behavior of PDADMA/PSS PEMs. Before thermal treatment, PDADMA-terminated PEMs swell more than PSS-terminated PEMs when exposed to humid air and water.[116] After thermal treatments, PEMs lost a portion of the total amount of swelling water present, depending on film thickness and terminating layer. This decrease is accompanied by a decrease in density of the PEM for thin films and an increase in density for thick PEMs. These effects are pronounced for PDADMA-terminated films.

6. Water microenvironments within polyelectrolyte complexes and multilayers

In the previous sections, we identified that water plays a key role in the structure, mechanical, and thermal properties of PECs and PEMs. Looking to the future, the mechanism by which water controls these features will be an area of intense interest. To-date, studies have examined the role of water content and water microenvironments within PECs. On the other hand, a large portion of PEC literature does not analyze or measure water content, thus preventing generalized comparisons of prior work. Looking to the future, it will be important to quantify the water content within the PEC so as to consider water's contributions to diffusion and dynamics appropriately. This is especially important for the consideration of solid- vs liquid-like PECs, in which liquid coacervates contain far more water.

Water may exist in different microenvironments within a PEC, such as in close contact with an ion pair or within voids. One of the earliest reports identifying water microenvironments in PEMs arose as a result of disparities in the swelling contributions of water obtained from both thickness and density measurements.[117] It was revealed that some water molecules are present within the voids in the PEM and the rest are associated with the polyelectrolyte chains. These studies were accomplished by observing the changes in the scattering length density (SLD), refractive index and thickness of PDADMA/PSS PEMs using ellipsometry and NR,[116-118] resulting in the void and extended void models. Similarly, MD simulations [119] have shown that water channels may be formed within PDADMA/PSS PECs. These water molecules were classified as "bulk" water that fills the channels and "surface" water that is in direct contact with PE chains. Other techniques, such as DSC and ATR-FTIR spectroscopy,[34, 96] have shown that water molecules exist in different microenvironments within both PEC and PEM structures.We have examined water microenvironments in PDADMA/PSS PECs using MDSC.[34] By monitoring the freezing point of water in PDADMA/PSS PECs of varying hydration levels (18 to 30 wt% water), different bound states of water were identified.[34] At lower hydration levels, < 30 wt%, there was no indication of melting or freezing of water during heating and cooling cycles. [34] At lower hydration levels, < 30 wt%, there was no indication of melting or freezing of water during heating and cooling cycles. This suggests that the water was in a tightly bound state which restricted mobility of the water molecules. This water was termed non-freezing bound water. At 30 wt % water, a transition peak was observed, but at a temperature less than the melting temperature of pure water (273 K). This was termed freezing bound water, indicating that the water was bound but loose enough that it could still freeze or melt. Water that melts at 273 K was termed freezing non-bound water. Such a water microenvironment is independent of the polymer chain interactions and acts as bulk water normally would. Within the hydration level studied, freezing non-bound water was not observed, suggesting that all water molecules were bound to the polyelectrolyte chains to varying extents.

Similar results on the microenvironments of water were obtained from direct observations of the OD stretch peak of PDADMA/PSS PEMs immersed in HOD using ATR-FTIR spectroscopy.[96] In this case, as prepared PEMs were exposed to varying concentrations of NaCl solutions made with 95:5 v/v H_2O:D_2O (HOD). Changes in the resulting OD stretch peak were monitored as a measure of hydrogen bonding variation in response to ionic strength and temperature. By deconvoluting each OD stretch peak, three possible water microenvironments were identified: high frequency water which is water in a tightly bound state with polyelectrolyte ion pairs; low frequency water which is loosely bound water; and bulk water which is free of the influence of ion pairs. In agreement with the prior MDSC study, no bulk water was found for all PEMs studied, indicating that all water molecules present in the PEM had some interactions with the polyelectrolyte ion pairs. An increase in temperature lead to a decrease in the low frequency water present in the PEM while high frequency water became more

tightly bound. Increase in ionic strength led to an increase in the amount of high frequency water in the PEMs.

Conclusions

Products of polyelectrolyte complexation (PEMs, PECs, coacervates) have gained interest for their potential impacts across a wide range of industries. With almost a century of research, much knowledge has been amassed on the nature of PECs. However, a comprehensive view of PECs remains lacking because of their highly complex and wide-ranging properties. The key features that most heavily influence a PEC's behaviour include the choice of system, water content, salt content, pH, and temperature. Emerging studies indicate that hydrophobicity of the system (as well as the solvents to which that system are exposed) affect resultant properties. Together, these features control whether the PEC is solid- or liquid-like, as well as glassy or rubbery. Ultimately, the physical properties are tied to understanding the number of ion pairs in the system, the strength of that ion pair, and its lifetime. We conclude here with several observations and recommendations for the readership.

First, in considering the PEC structure, it is important to recognize that polycations and polyanions are often arranged in a "3D scrambled egg structure", in which a polycation may be involved with multiple polyelectrolyte chains. This notion is counter to popular drawings of PECs, in which a single polyanion matches a single polycation in a ladder-type arrangement. Further, within the complex, the number of intrinsic ion pairs per chain or the doping level "y" for both positive and negative polyelectrolytes is not always equivalent due to compositional mismatch between the polyelectrolytes. Therefore, we recommend considering y^+ and y^- to more accurately describe the true doping levels. Also, at very high ionic strengths, the salt ions may exist as co-ions, complicating the understanding of the PEC structure. A better understanding of the polyelectrolyte complex structure at the molecular level is needed.

As for theory, many have been applied with the aim of fully describing the liquid-like coacervate/solution boundary. However, the coacervate-precipitate boundary remains ill-defined. Additionally, there is a lack of agreement between theoretical models and experimental results related to salt partitioning between polymer-rich and polymer-deficient phases. Theoretical frameworks that address both the coacervate/solution and precipitate/coacervate boundaries are needed, especially those that account for salt and water fraction.

Regarding chain diffusion within PECs, most work has focused upon PEMs. Due to the nature of assembly, chain diffusion in PEMs is anisotropic in nature; thus, the direction of the measured diffusion coefficient (parallel or perpendicular) depends on the experimental technique employed. Further, depending on the technique utilized, the diffusion coefficient measured may be assigned to either diffusion of the chain or of extrinsic sites. Much less is known about chain diffusion within PECs, which may be consider isotropic. Efforts are still required to understand the nature and mechanism of diffusion in PECs and PEMs and whether relaxation of one chain cascades to the other and subsequently to the entire PEM.

With respect to the rheology of PECs, significant advancements have been made in recent years. A growing body of work focuses upon applying various superposition principles to time, temperature, salt, pH, and water. Specifically, salt superpositioning and long-term relaxation in coacervates has been explained using sticky Rouse and sticky-reptation models. Because polymer volume fraction changes with salt concentration it may be important to consider its impact on relaxation time, thus affecting interpretations of time-salt-superpositioning. To gain a better understanding of the impact of salt and water on mechanical properties we recommend that the PEC's polyelectrolyte ratio, doping level (y^+, y^-) and water content be quantified and reported so that the intrinsic ion pair fraction and polymer volume fraction can be estimated. Ultimately, the latter two features influence the number of sticker sites as well as the density of the system, which are relevant to rheological models. Notably, an increasing number of superpositioned rheological graphs are invoking a vertical shift factor, "b". We recommend that vertical shifting be considered in connection to a physical phenomenon, possibly to changes in the polymer volume fraction or changes in density of the system. Even though long-term relaxation times in PECs have been explained using sticky Rouse and sticky-reptation models, a robust theoretical explanation regarding the observed glassy behavior in PECs is still needed.

Finally, the role of water has been emerging as an important factor in the glass transition temperature and the dynamics of PECs. Water provides lubrication and plasticization to tightly bound dry PEC structures, enabling a glass transition with increasing water content. More studies are necessary to fully understand the relationship between water and the T_g because the current understanding is phenomenologically driven. Also of note, water may exist within different microevironments within the PEC, affecting different aspects of the physical behaviour. We recommend considering these microenvironments and characterizing them to understand the relative amounts of bound, loose, or bulk water within the PEC. Mixed solvent systems may also be of interest to examine hydrophobic effects. Lastly, due to the longer relaxation times observed in solid PECs, as-prepared solid PECs may exist in a kinetically trapped state; therefore, considering the solid PEC's thermomechanical history, its annealing (at $T > T_g$) to remove any residual stresses or approach an equilibrium structure, as well as its processing conditions should be considered. There remains a need to recognize and study these systems as non-equilibrium structures.

Past work on PECs and PEMs has culminated in a finer understanding of the fundamental dynamics of these fascinating structures. Looking to the future, there remains a rich landscape for investigation, particularly in theory and modelling, aided by the experimental quantification of the PEC structure and its dynamic properties.

Conflicts of interest

There are no conflicts to declare.

Acknowledgements

This work is supported by the National Science Foundation under Grant No. 1905732. We thank Drs. Maria Sammalkorpi (Aalto University) and Piotr Batys (Polish Academy of Sciences) for their helpful discussions.

Notes and references

1. de Jong, B., Coacervation. *Proc. Royal Acad. Amsterdam* **1929,** *32*, 849-856.
2. Jong, H. G.; Kruyt, H. R., Coacervation (partial miscibility in colloid systems). *Proc. K. Ned. Akad. Wet.* **1929,** *32*, 849-856.
3. Huang, S.; Zhao, M.; Dawadi, M. B.; Cai, Y.; Lapitsky, Y.; Modarelli, D. A.; Zacharia, N. S., Effect of small molecules on the phase behavior and coacervation of aqueous solutions of poly(diallyldimethylammonium chloride) and poly(sodium 4-styrene sulfonate). *Journal of Colloid and Interface Science* **2018,** *518*, 216-224.
4. Wang, Q.; Schlenoff, J. B., The Polyelectrolyte Complex/Coacervate Continuum. *Macromolecules* **2014,** *47* (9), 3108-3116.
5. Ali, S.; Prabhu, V. M., Relaxation Behavior by Time-Salt and Time-Temperature Superpositions of Polyelectrolyte Complexes from Coacervate to Precipitate. *Gels* **2018,** *4* (1), 11.
6. Zhang, R.; Zhang, Y.; Antila, H. S.; Lutkenhaus, J. L.; Sammalkorpi, M., Role of Salt and Water in the Plasticization of PDAC/PSS Polyelectrolyte Assemblies. *The Journal of Physical Chemistry B* **2017,** *121* (1), 322-333.
7. Riback, J. A.; Zhu, L.; Ferrolino, M. C.; Tolbert, M.; Mitrea, D. M.; Sanders, D. W.; Wei, M.-T.; Kriwacki, R. W.; Brangwynne, C. P., Composition-dependent thermodynamics of intracellular phase separation. *Nature* **2020,** *581* (7807), 209-214.
8. Shao, H.; Bachus, K. N.; Stewart, R. J., A water-borne adhesive modeled after the sandcastle glue of P. californica. *Macromol Biosci* **2009,** *9* (5), 464-471.
9. Meka, V. S.; Sing, M. K. G.; Pichika, M. R.; Nali, S. R.; Kolapalli, V. R. M.; Kesharwani, P., A comprehensive review on polyelectrolyte complexes. *Drug Discovery Today* **2017,** *22* (11), 1697-1706.
10. Zhao, S.; Caruso, F.; Dähne, L.; Decher, G.; De Geest, B. G.; Fan, J.; Feliu, N.; Gogotsi, Y.; Hammond, P. T.; Hersam, M. C.; Khademhosseini, A.; Kotov, N.; Leporatti, S.; Li, Y.; Lisdat, F.; Liz-Marzán, L. M.; Moya, S.; Mulvaney, P.; Rogach, A. L.; Roy, S.; Shchukin, D. G.; Skirtach, A. G.; Stevens, M. M.; Sukhorukov, G. B.; Weiss, P. S.; Yue, Z.; Zhu, D.; Parak, W. J., The Future of Layer-by-Layer Assembly: A Tribute to ACS Nano Associate Editor Helmuth Möhwald. *ACS Nano* **2019**.
11. Zhang, Y.; Yildirim, E.; Antila, H. S.; Valenzuela, L. D.; Sammalkorpi, M.; Lutkenhaus, J. L., The influence of ionic strength and mixing ratio on the colloidal stability of PDAC/PSS polyelectrolyte complexes. *Soft Matter* **2015,** *11* (37), 7392-7401.
12. Tirrell, M., Polyelectrolyte Complexes: Fluid or Solid? *ACS Central Science* **2018,** *4* (5), 532-533.
13. Chollakup, R.; Smitthipong, W.; Eisenbach, C. D.; Tirrell, M., Phase Behavior and Coacervation of Aqueous Poly(acrylic acid)−Poly(allylamine) Solutions. *Macromolecules* **2010,** *43* (5), 2518-2528.
14. Kayitmazer, A. B., Thermodynamics of complex coacervation. *Advances in Colloid and Interface Science* **2017,** *239*, 169-177.
15. Sing, C. E.; Perry, S. L., Recent progress in the science of complex coacervation. *Soft Matter* **2020**.
16. Schaaf, P.; Schlenoff, J. B., Saloplastics: Processing Compact Polyelectrolyte Complexes. *Advanced Materials* **2015,** *27* (15), 2420-2432.
17. Michaels, A. S., POLYELECTROLYTE COMPLEXES. *Industrial & Engineering Chemistry* **1965,** *57* (10), 32-40.
18. Turgeon, S. L.; Schmitt, C.; Sanchez, C., Protein–polysaccharide complexes and coacervates. *Current Opinion in Colloid & Interface Science* **2007,** *12* (4), 166-178.
19. Schlenoff, J. B.; Rmaile, A. H.; Bucur, C. B., Hydration Contributions to Association in Polyelectrolyte Multilayers and Complexes: Visualizing Hydrophobicity. *Journal of the American Chemical Society* **2008,** *130* (41), 13589-13597.
20. Zhang, Y.; Batys, P.; O'Neal, J. T.; Li, F.; Sammalkorpi, M.; Lutkenhaus, J. L., Molecular Origin of the Glass Transition in Polyelectrolyte Assemblies. *ACS Central Science* **2018,** *4* (5), 638-644.
21. Fu, J.; Fares, H. M.; Schlenoff, J. B., Ion-Pairing Strength in Polyelectrolyte Complexes. *Macromolecules* **2017,** *50* (3), 1066-1074.
22. Schlenoff, J. B.; Yang, M.; Digby, Z. A.; Wang, Q., Ion Content of Polyelectrolyte Complex Coacervates and the Donnan Equilibrium. *Macromolecules* **2019,** *52* (23), 9149-9159.
23. Vögele, M.; Holm, C.; Smiatek, J., Coarse-grained simulations of polyelectrolyte complexes: MARTINI models for poly(styrene sulfonate) and poly(diallyldimethylammonium). *The Journal of Chemical Physics* **2015,** *143* (24), 243151.
24. Farhat, T. R.; Schlenoff, J. B., Doping-Controlled Ion Diffusion in Polyelectrolyte Multilayers: Mass Transport in Reluctant Exchangers. *Journal of the American Chemical Society* **2003,** *125* (15), 4627-4636.
25. Farhat, T. R.; Schlenoff, J. B., Ion Transport and Equilibria in Polyelectrolyte Multilayers. *Langmuir* **2001,** *17* (4), 1184-1192.
26. Ghostine, R. A.; Jisr, R. M.; Lehaf, A.; Schlenoff, J. B., Roughness and Salt Annealing in a Polyelectrolyte Multilayer. *Langmuir* **2013,** *29* (37), 11742-11750.
27. McAloney, R. A.; Dudnik, V.; Goh, M. C., Kinetics of Salt-Induced Annealing of a Polyelectrolyte Multilayer Film Morphology. *Langmuir* **2003,** *19* (9), 3947-3952.
28. Krebs, T.; Tan, H. L.; Andersson, G.; Morgner, H.; Gregory Van Patten, P., Increased layer interdiffusion in polyelectrolyte films upon annealing in water and aqueous salt solutions. *Physical chemistry chemical physics : PCCP* **2006,** *8* (46), 5462-8.
29. O'Neal, J. T.; Dai, E. Y.; Zhang, Y.; Clark, K. B.; Wilcox, K. G.; George, I. M.; Ramasamy, N. E.; Enriquez, D.; Batys, P.; Sammalkorpi, M.; Lutkenhaus, J. L., QCM-D Investigation of Swelling Behavior of Layer-by-Layer Thin Films upon Exposure to Monovalent Ions. *Langmuir* **2018,** *34* (3), 999-1009.
30. Suarez-Martinez, P. C.; Batys, P.; Sammalkorpi, M.; Lutkenhaus, J. L., Time–Temperature and Time–Water Superposition Principles Applied to Poly(allylamine)/Poly(acrylic acid) Complexes. *Macromolecules* **2019,** *52* (8), 3066-3074.
31. Michaels, A. S.; Miekka, R. G., POLYCATION-POLYANION COMPLEXES: PREPARATION AND PROPERTIES OF POLY-(VINYLBENZYLTRIMETHYLAMMONIUM) POLY-(STYRENESULFONATE). *The Journal of Physical Chemistry* **1961,** *65* (10), 1765-1773.

32. Lazutin, A. A.; Semenov, A. N.; Vasilevskaya, V. V., Polyelectrolyte Complexes Consisting of Macromolecules With Varied Stiffness: Computer Simulation. *Macromolecular Theory and Simulations* **2012,** *21* (5), 328-339.
33. Spruijt, E.; Leermakers, F. A. M.; Fokkink, R.; Schweins, R.; van Well, A. A.; Cohen Stuart, M. A.; van der Gucht, J., Structure and Dynamics of Polyelectrolyte Complex Coacervates Studied by Scattering of Neutrons, X-rays, and Light. *Macromolecules* **2013,** *46* (11), 4596-4605.
34. Batys, P.; Zhang, Y.; Lutkenhaus, J. L.; Sammalkorpi, M., Hydration and Temperature Response of Water Mobility in Poly(diallyldimethylammonium)–Poly(sodium 4-styrenesulfonate) Complexes. *Macromolecules* **2018,** *51* (20), 8268-8277.
35. Jeon, J.; Dobrynin, A. V., Molecular Dynamics Simulations of Polyelectrolyte−Polyampholyte Complexes. Effect of Solvent Quality and Salt Concentration. *The Journal of Physical Chemistry B* **2006,** *110* (48), 24652-24665.
36. Delaney, K. T.; Fredrickson, G. H., Theory of polyelectrolyte complexation—Complex coacervates are self-coacervates. *The Journal of Chemical Physics* **2017,** *146* (22), 224902.
37. Li, L.; Srivastava, S.; Andreev, M.; Marciel, A. B.; de Pablo, J. J.; Tirrell, M. V., Phase Behavior and Salt Partitioning in Polyelectrolyte Complex Coacervates. *Macromolecules* **2018,** *51* (8), 2988-2995.
38. Overbeek, J. T. G.; Voorn, M. J., Phase separation in polyelectrolyte solutions. Theory of complex coacervation. *Journal of Cellular and Comparative Physiology* **1957,** *49* (S1), 7-26.
39. Voorn, M. J., Complex coacervation. I. General theoretical considerations. *Recueil des Travaux Chimiques des Pays-Bas* **1956,** *75* (3), 317-330.
40. Jha, P. K.; Desai, P. S.; Li, J.; Larson, R. G., pH and Salt Effects on the Associative Phase Separation of Oppositely Charged Polyelectrolytes. *Polymers* **2014,** *6* (5), 1414-1436.
41. Salehi, A.; Desai, P. S.; Li, J.; Steele, C. A.; Larson, R. G., Relationship between Polyelectrolyte Bulk Complexation and Kinetics of Their Layer-by-Layer Assembly. *Macromolecules* **2015,** *48* (2), 400-409.
42. Lou, J.; Friedowitz, S.; Qin, J.; Xia, Y., Tunable Coacervation of Well-Defined Homologous Polyanions and Polycations by Local Polarity. *ACS Central Science* **2019,** *5* (3), 549-557.
43. Zhang, P.; Shen, K.; Alsaifi, N. M.; Wang, Z.-G., Salt Partitioning in Complex Coacervation of Symmetric Polyelectrolytes. *Macromolecules* **2018,** *51* (15), 5586-5593.
44. Perry, S. L.; Sing, C. E., PRISM-Based Theory of Complex Coacervation: Excluded Volume versus Chain Correlation. *Macromolecules* **2015,** *48* (14), 5040-5053.
45. Kudlay, A.; Ermoshkin, A. V.; Olvera de la Cruz, M., Complexation of Oppositely Charged Polyelectrolytes: Effect of Ion Pair Formation. *Macromolecules* **2004,** *37* (24), 9231-9241.
46. Kudlay, A.; Cruz, M. O. d. l., Precipitation of oppositely charged polyelectrolytes in salt solutions. *The Journal of Chemical Physics* **2004,** *120* (1), 404-412.
47. Zhang, P.; Alsaifi, N. M.; Wu, J.; Wang, Z.-G., Polyelectrolyte complex coacervation: Effects of concentration asymmetry. *The Journal of Chemical Physics* **2018,** *149* (16), 163303.
48. Adhikari, S.; Leaf, M. A.; Muthukumar, M., Polyelectrolyte complex coacervation by electrostatic dipolar interactions. *The Journal of Chemical Physics* **2018,** *149* (16), 163308.
49. Spruijt, E.; Westphal, A. H.; Borst, J. W.; Cohen Stuart, M. A.; van der Gucht, J., Binodal Compositions of Polyelectrolyte Complexes. *Macromolecules* **2010,** *43* (15), 6476-6484.
50. Sing, C. E., Development of the modern theory of polymeric complex coacervation. *Advances in Colloid and Interface Science* **2017,** *239*, 2-16.
51. Liu, Y.; Momani, B.; Winter, H. H.; Perry, S. L., Rheological characterization of liquid-to-solid transitions in bulk polyelectrolyte complexes. *Soft Matter* **2017,** *13* (40), 7332-7340.
52. Meng, S.; Liu, Y.; Yeo, J.; Ting, J. M.; Tirrell, M. V., Effect of mixed solvents on polyelectrolyte complexes with salt. *Colloid and Polymer Science* **2020**.
53. Pristinski, D.; Kozlovskaya, V.; Sukhishvili, S. A., Fluorescence correlation spectroscopy studies of diffusion of a weak polyelectrolyte in aqueous solutions. *The Journal of Chemical Physics* **2004,** *122* (1), 014907.
54. Xu, L.; Selin, V.; Zhuk, A.; Ankner, J. F.; Sukhishvili, S. A., Molecular Weight Dependence of Polymer Chain Mobility within Multilayer Films. *ACS Macro Letters* **2013,** *2* (10), 865-868.
55. Xu, L.; Pristinski, D.; Zhuk, A.; Stoddart, C.; Ankner, J. F.; Sukhishvili, S. A., Linear versus Exponential Growth of Weak Polyelectrolyte Multilayers: Correlation with Polyelectrolyte Complexes. *Macromolecules* **2012,** *45* (9), 3892-3901.
56. Selin, V.; Ankner, J. F.; Sukhishvili, S. A., Diffusional Response of Layer-by-Layer Assembled Polyelectrolyte Chains to Salt Annealing. *Macromolecules* **2015,** *48* (12), 3983-3990.
57. Xu, L.; Kozlovskaya, V.; Kharlampieva, E.; Ankner, J. F.; Sukhishvili, S. A., Anisotropic Diffusion of Polyelectrolyte Chains within Multilayer Films. *ACS Macro Lett* **2011,** *2012* (1), 127-130.
58. Nazaran, P.; Bosio, V.; Jaeger, W.; Anghel, D. F.; v. Klitzing, R., Lateral Mobility of Polyelectrolyte Chains in Multilayers. *The Journal of Physical Chemistry B* **2007,** *111* (29), 8572-8581.
59. Jomaa, H. W.; Schlenoff, J. B., Salt-Induced Polyelectrolyte Interdiffusion in Multilayered Films: A Neutron Reflectivity Study. *Macromolecules* **2005,** *38* (20), 8473-8480.
60. Dubas, S. T.; Schlenoff, J. B., Swelling and Smoothing of Polyelectrolyte Multilayers by Salt. *Langmuir* **2001,** *17* (25), 7725-7727.
61. Soltwedel, O.; Nestler, P.; Neumann, H.-G.; Paßvogel, M.; Köhler, R.; Helm, C. A., Influence of Polycation (PDADMAC) Weight on Vertical Diffusion within Polyelectrolyte Multilayers during Film Formation and Postpreparation Treatment. *Macromolecules* **2012,** *45* (19), 7995-8004.
62. Soltwedel, O.; Ivanova, O.; Nestler, P.; Müller, M.; Köhler, R.; Helm, C. A., Interdiffusion in Polyelectrolyte Multilayers. *Macromolecules* **2010,** *43* (17), 7288-7293.
63. Sill, A.; Nestler, P.; Azinfar, A.; Helm, C. A., Tailorable Polyanion Diffusion Coefficient in LbL Films: The Role of Polycation Molecular Weight and Polymer Conformation. *Macromolecules* **2019,** *52* (22), 9045-9052.
64. Zan, X.; Peng, B.; Hoagland, D. A.; Su, Z., Polyelectrolyte uptake by PEMs: Impact of salt concentration. *Polymer Chemistry* **2011,** *2* (11).
65. Zan, X.; Hoagland, D. A.; Wang, T.; Peng, B.; Su, Z., Polyelectrolyte uptake by PEMs: Impacts of molecular weight and counterion. *Polymer* **2012,** *53* (22), 5109-5115.
66. Fares, H. M.; Schlenoff, J. B., Diffusion of Sites versus Polymers in Polyelectrolyte Complexes and Multilayers. *J Am Chem Soc* **2017,** *139* (41), 14656-14667.
67. Kharlampieva, E.; Ankner, J. F.; Rubinstein, M.; Sukhishvili, S. A., pH-induced release of polyanions from multilayer films. *Phys Rev Lett* **2008,** *100* (12), 128303.
68. Yoo, P. J.; Zacharia, N. S.; Doh, J.; Nam, K. T.; Belcher, A. M.; Hammond, P. T., Controlling Surface Mobility in Interdiffusing Polyelectrolyte Multilayers. *ACS Nano* **2008,** *2* (3), 561-571.

69. Spruijt, E.; Sprakel, J.; Lemmers, M.; Stuart, M. A.; van der Gucht, J., Relaxation dynamics at different time scales in electrostatic complexes: time-salt superposition. *Phys Rev Lett* **2010,** *105* (20), 208301.
70. Guzmán, E.; Ritacco, H.; Rubio, J. E. F.; Rubio, R. G.; Ortega, F., Salt-induced changes in the growth of polyelectrolyte layers of poly(diallyl-dimethylammonium chloride) and poly(4-styrene sulfonate of sodium). *Soft Matter* **2009,** *5* (10).
71. Yang, M.; Shi, J.; Schlenoff, J. B., Control of Dynamics in Polyelectrolyte Complexes by Temperature and Salt. *Macromolecules* **2019,** *52* (5), 1930-1941.
72. Tekaat, M.; Butergerds, D.; Schonhoff, M.; Fery, A.; Cramer, C., Scaling properties of the shear modulus of polyelectrolyte complex coacervates: a time-pH superposition principle. *Phys Chem Chem Phys* **2015,** *17* (35), 22552-6.
73. Sadman, K.; Wang, Q.; Chen, Y.; Keshavarz, B.; Jiang, Z.; Shull, K. R., Influence of Hydrophobicity on Polyelectrolyte Complexation. *Macromolecules* **2017,** *50* (23), 9417-9426.
74. Dubin, P. L.; Li, Y.; Jaeger, W., Mesophase Separation in Polyelectrolyte-Mixed Micelle Coacervates. *Langmuir* **2008,** *24* (9), 4544-4549.
75. Huang, W.; Li, J.; Liu, D.; Tan, S.; Zhang, P.; Zhu, L.; Yang, S., Polyelectrolyte Complex Fiber of Alginate and Poly(diallyldimethylammonium chloride): Humidity Induced Mechanical Transition and Shape Memory. *ACS Applied Polymer Materials* **2020**.
76. Akkaoui, K.; Yang, M.; Digby, Z. A.; Schlenoff, J. B., Ultraviscosity in Entangled Polyelectrolyte Complexes and Coacervates. *Macromolecules* **2020**.
77. Shamoun, R. F.; Hariri, H. H.; Ghostine, R. A.; Schlenoff, J. B., Thermal Transformations in Extruded Saloplastic Polyelectrolyte Complexes. *Macromolecules* **2012,** *45* (24), 9759-9767.
78. Ali, S.; Prabhu, V. M., Relaxation Behavior by Time-Salt and Time-Temperature Superpositions of Polyelectrolyte Complexes from Coacervate to Precipitate. *Gels* **2018,** *4* (1).
79. Hamad, F. G.; Chen, Q.; Colby, R. H., Linear Viscoelasticity and Swelling of Polyelectrolyte Complex Coacervates. *Macromolecules* **2018,** *51* (15), 5547-5555.
80. Rouse, P. E., A Theory of the Linear Viscoelastic Properties of Dilute Solutions of Coiling Polymers. *The Journal of Chemical Physics* **1953,** *21* (7), 1272-1280.
81. Hiemenz, P. C.; Lodge, T. P., *Polymer Chemistry*. CRC press, Taylor & Francis Group: Boca Raton, FL, 2007; p 419-460, 486-488.
82. Rubinstein, M.; Colby, R. H., *Polymer Physics*. Oxford University Press: Oxford, 2003; p 309-390.
83. Zhang, Z.; Chen, Q.; Colby, R. H., Dynamics of associative polymers. *Soft Matter* **2018,** *14* (16), 2961-2977.
84. Green, M. S.; Tobolsky, A. V., A New Approach to the Theory of Relaxing Polymeric Media. *The Journal of Chemical Physics* **1946,** *14* (2), 80-92.
85. Rubinstein, M.; Semenov, A. N., Thermoreversible Gelation in Solutions of Associating Polymers. 2. Linear Dynamics. *Macromolecules* **1998,** *31* (4), 1386-1397.
86. de Gennes, P. G., Reptation of a Polymer Chain in the Presence of Fixed Obstacles. *The Journal of Chemical Physics* **1971,** *55* (2), 572-579.
87. Rubinstein, M.; Semenov, A. N., Dynamics of Entangled Solutions of Associating Polymers. *Macromolecules* **2001,** *34* (4), 1058-1068.
88. Spruijt, E.; Cohen Stuart, M. A.; van der Gucht, J., Linear Viscoelasticity of Polyelectrolyte Complex Coacervates. *Macromolecules* **2013,** *46* (4), 1633-1641.
89. TA instruments *Dynamic Mechanical Analysis: Basic Theory & Applications Training*; TA instruments: 2018; p 202.
90. Dealy, J.; Plazek, D., Time-temperature superposition-a users guide. *Rheol. Bull.* **2009,** *78*, 16-31.
91. Imre, A. W.; Schonhoff, M.; Cramer, C., Unconventional scaling of electrical conductivity spectra for PSS-PDADMAC polyelectrolyte complexes. *Phys Rev Lett* **2009,** *102* (25), 255901.
92. De, S.; Ostendorf, A.; Schonhoff, M.; Cramer, C., Ion Conduction and Its Activation in Hydrated Solid Polyelectrolyte Complexes. *Polymers (Basel)* **2017,** *9* (11).
93. Marciel, A. B.; Srivastava, S.; Tirrell, M. V., Structure and rheology of polyelectrolyte complex coacervates. *Soft Matter* **2018,** *14* (13), 2454-2464.
94. Priftis, D.; Megley, K.; Laugel, N.; Tirrell, M., Complex coacervation of poly(ethylene-imine)/polypeptide aqueous solutions: thermodynamic and rheological characterization. *J Colloid Interface Sci* **2013,** *398*, 39-50.
95. Dompé, M.; Vahdati, M.; van Ligten, F.; Cedano-Serrano, F. J.; Hourdet, D.; Creton, C.; Zanetti, M.; Bracco, P.; van der Gucht, J.; Kodger, T.; Kamperman, M., Enhancement of the Adhesive Properties by Optimizing the Water Content in PNIPAM-Functionalized Complex Coacervates. *ACS Applied Polymer Materials* **2020,** *2* (4), 1722-1730.
96. Eneh, C. I.; Bolen, M. J.; Suarez-Martinez, P. C.; Bachmann, A. L.; Zimudzi, T. J.; Hickner, M. A.; Batys, P.; Sammalkorpi, M.; Lutkenhaus, J. L., Fourier transform infrared spectroscopy investigation of water microenvironments in polyelectrolyte multilayers at varying temperatures. *Soft Matter* **2020,** *16* (9), 2291-2300.
97. Batys, P.; Zhang, Y.; Lutkenhaus, J. L.; Sammalkorpi, M., Hydration and Temperature Response of Water Mobility in Poly(diallyldimethylammonium)-Poly(sodium 4-styrenesulfonate) Complexes. *Macromolecules* **2018,** *51* (20), 8268-8277.
98. Batys, P.; Kivisto, S.; Lalwani, S. M.; Lutkenhaus, J. L.; Sammalkorpi, M., Comparing water-mediated hydrogen-bonding in different polyelectrolyte complexes. *Soft Matter* **2019,** *15* (39), 7823-7831.
99. Cramer, C.; De, S.; Schonhoff, M., Time-humidity-superposition principle in electrical conductivity spectra of ion-conducting polymers. *Phys Rev Lett* **2011,** *107* (2), 028301.
100. Huang, J.; Morin, F. J.; Laaser, J. E., Charge-Density-Dominated Phase Behavior and Viscoelasticity of Polyelectrolyte Complex Coacervates. *Macromolecules* **2019,** *52* (13), 4957-4967.
101. Zhang, Y.; Li, F.; Valenzuela, L. D.; Sammalkorpi, M.; Lutkenhaus, J. L., Effect of Water on the Thermal Transition Observed in Poly(allylamine hydrochloride)–Poly(acrylic acid) Complexes. *Macromolecules* **2016,** *49* (19), 7563-7570.
102. Yildirim, E.; Zhang, Y.; Lutkenhaus, J. L.; Sammalkorpi, M., Thermal Transitions in Polyelectrolyte Assemblies Occur via a Dehydration Mechanism. *ACS Macro Letters* **2015,** *4* (9), 1017-1021.
103. Fu, J.; Abbett, R. L.; Fares, H. M.; Schlenoff, J. B., Water and the Glass Transition Temperature in a Polyelectrolyte Complex. *ACS Macro Letters* **2017,** *6* (10), 1114-1118.
104. Yano, O.; Wada, Y., Effect of sorbed water on dielectric and mechanical properties of polyion complex. *Journal of Applied Polymer Science* **1980,** *25* (8), 1723-1735.
105. Shao, L.; Lutkenhaus, J. L., Thermochemical properties of free-standing electrostatic layer-by-layer assemblies containing poly(allylamine hydrochloride) and poly(acrylic acid). *Soft Matter* **2010,** *6* (14), 3363-3369.
106. Lyu, X.; Clark, B.; Peterson, A. M., Thermal transitions in and structures of dried polyelectrolytes and polyelectrolyte

complexes. *Journal of Polymer Science Part B: Polymer Physics* **2017,** *55* (8), 684-691.
107. Vidyasagar, A.; Sung, C.; Gamble, R.; Lutkenhaus, J. L., Thermal Transitions in Dry and Hydrated Layer-by-Layer Assemblies Exhibiting Linear and Exponential Growth. *ACS Nano* **2012,** *6* (7), 6174-6184.
108. Vidyasagar, A.; Sung, C.; Losensky, K.; Lutkenhaus, J. L., pH-Dependent Thermal Transitions in Hydrated Layer-by-Layer Assemblies Containing Weak Polyelectrolytes. *Macromolecules* **2012,** *45* (22), 9169-9176.
109. Kang, E.; Kim, H.; Gray, L. A. G.; Christie, D.; Jonas, U.; Graczykowski, B.; Furst, E. M.; Priestley, R. D.; Fytas, G., Ultrathin Shell Layers Dramatically Influence Polymer Nanoparticle Surface Mobility. *Macromolecules* **2018,** *51* (21), 8522-8529.
110. Sung, C.; Hearn, K.; Lutkenhaus, J., Thermal transitions in hydrated layer-by-layer assemblies observed using electrochemical impedance spectroscopy. *Soft Matter* **2014,** *10* (34), 6467-6476.
111. Zerball, M.; Laschewsky, A.; Köhler, R.; Von Klitzing, R., The Effect of Temperature Treatment on the Structure of Polyelectrolyte Multilayers. *Polymers* **2016,** *8* (4), 120.
112. Diamanti, E.; Muzzio, N.; Gregurec, D.; Irigoyen, J.; Pasquale, M.; Azzaroni, O.; Brinkmann, M.; Moya, S. E., Impact of thermal annealing on wettability and antifouling characteristics of alginate poly-l-lysine polyelectrolyte multilayer films. *Colloids and Surfaces B: Biointerfaces* **2016,** *145*, 328-337.
113. Steitz, R.; Leiner, V.; Tauer, K.; Khrenov, V.; v. Klitzing, R., Temperature-induced changes in polyelectrolyte films at the solid–liquid interface. *Applied Physics A* **2002,** *74* (1), s519-s521.
114. Köhler, K.; Shchukin, D. G.; Möhwald, H.; Sukhorukov, G. B., Thermal Behavior of Polyelectrolyte Multilayer Microcapsules. 1. The Effect of Odd and Even Layer Number. *The Journal of Physical Chemistry B* **2005,** *109* (39), 18250-18259.
115. Kim, B.-S.; Fan, T.-H.; Vinogradova, O. I., Thermal softening of superswollen polyelectrolyte microcapsules. *Soft Matter* **2011,** *7* (6), 2705-2708.
116. Zerball, M.; Laschewsky, A.; von Klitzing, R., Swelling of Polyelectrolyte Multilayers: The Relation Between, Surface and Bulk Characteristics. *The Journal of Physical Chemistry B* **2015,** *119* (35), 11879-11886.
117. Dodoo, S.; Steitz, R.; Laschewsky, A.; von Klitzing, R., Effect of ionic strength and type of ions on the structure of water swollen polyelectrolyte multilayers. *Physical Chemistry Chemical Physics* **2011,** *13* (21), 10318-10325.
118. Löhmann, O.; Zerball, M.; von Klitzing, R., Water Uptake of Polyelectrolyte Multilayers Including Water Condensation in Voids. *Langmuir* **2018,** *34* (38), 11518-11525.
119. Diddens, D.; Baschnagel, J.; Johner, A., Microscopic Structure of Compacted Polyelectrolyte Complexes: Insights from Molecular Dynamics Simulations. *ACS Macro Letters* **2019,** *8* (2), 123-127.